



An-Najah National University
Faculty of Graduate Studies

KINETICS, MECHANISM AND ANALYTICAL APPLICATION OF CYANIDE ABSTRACTION FROM HEXACYANOFERRATE [II] BY MERCURY [II] IN THE PRESENCE OF FERENE S

BY:

Imad Abdel Mun'em Mahmoud Harb

SUPERVISED BY:

Prof. Bassem F. Shraydeh

*Submitted in the partial fulfillment of the requirement for the
degree of Master of Science in Chemistry*

**An-Najah National University
Faculty of Graduate Studies
Department of Chemistry
Nablus – West Bank**

June, 2000

KINETICS, MECHANISM AND ANALYTICAL APPLICATION OF CYANIDE ABSTRACTION FROM HEXACYANOFERRATE [II] BY MERCURY [II] IN THE PRESENCE OF FERENE S

By

Imad Abdel Mun'em Mahmoud Harb

The examining committee considers this thesis satisfactory and acceptable for the award of master degree in Chemistry on 13 / 6 / 2000

Committee member

Signature

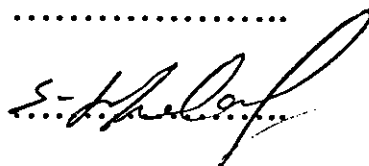
1. Prof. Bassem Shraydeh

.....

3. Dr. Fouad Bannoura

.....

2. Dr. Shukri Khalaf



This thesis was done under the supervision of Professor Bassem Shraydeh.



III

Acknowledgments

First of all, the author wishes to express his sincere appreciation to his supervisor Professor Bassem Shraydeh for his guidance, encouragement, constant care and help throughout the research work.

Thanks are also for the technical staff in laboratories of the Departments of Agriculture and Chemistry at An-Najah National University

Besides my colleagues at "Dora Al Qare' Basic Mixed School". I would like to thank heartily the headmaster of the School Mr. Bassam Abdel-mun'em Al Haj for his help and cooperation.

Finally, I would like to thank my parents, brothers, sisters, friends, colleagues, and students for their encouragement throughout my study and research.

Imad A. Harb

ملخص

تتناول هذه الدراسة حركية تفاعل استخلاص السيانيد (CN) من المركب المعقد سداسي سيانيد الحديد (II) البوتاسي $[K_4Fe(CN)_6]$ بواسطة العامل المساعد كلوريد الزئبق (II) في الوسط المائي وبوجود المتصلة (Ligand) الفرين أس $[Ferene S]$ ، حيث تم تتبع سير التفاعل باستخدام جهاز الطيف الضوئي على الموجة 593 nm بتتبع التغيرات الطارئة على امتصاص المركب المعقد ذو اللون الأزرق المتكون بين أيون الحديد (II) والمتصلة الفرين $[Ferene S]$.

إن التفاعل بين سداسي سيانيد الحديد (II) و متصلة الفرين بطيء جداً ، ولكن وبوجود كمية ضئيلة جداً من الزئبق (II) يتم التفاعل خلال بضع دقائق. هذا وقد تم دراسة أثر كل من درجة الحموضة، درجة الحرارة، تركيز كل من المواد المتفاعلة على سرعة التفاعل.

لقد تبين أن رتبة التفاعل من الدرجة الأولى بالنسبة لكل من سداسي سيانيد الحديد (II) و متصلة الفرين. وأيون الزئبق (II).

وقد تم حساب ثوابت معدلات التفاعل و المتغيرات الترموديناميكية. أيضاً لقد تم اقتراح مكنائكية (Mechanism) تفسر عملية التفاعل.

وأخيراً، تم اقتراح طريقة تحليلية حركية حساسة لإيجاد نسب ضئيلة من الزئبق في عينات دوائية.

Abstract

The kinetics of cyanide abstraction from potassium hexacyanoferrate (II) by mercuric chloride in the presence of the ligand Ferene S in aqueous solutions have been investigated spectrophotometrically by measuring the change in the absorbance of the blue Ferene-ferrous complex at 593 nm.

The reaction rate between potassium hexacyanoferrate (II) and Ferene is dramatically a slow process, while in presence of a trace amount of mercury(II) the reaction tends to completion within few minutes. Effect of pH, temperature, hexacyanoferrate (II), Ferene S, and mercury(II) concentrations on the rate of the reaction have been investigated.

The order of the reaction has been found to be first order with respect to potassium hexacyanoferrate (II), Ferene S, and mercury(II) chloride. Activation parameters for both the catalysed and the uncatalysed reactions have been calculated. A proposed mechanism that could explain the results has been suggested.

A kinetic method for mercury determination in medicinal samples has been proposed.

Table of contents

Committee Decision	I
Dedication	II
Acknowledgment	III
Abstract (Arabic)	IV
Abstract (English)	V
Table of Contents	VI
List of Tables	VIII
List of Figures	X

Chapter One: Introduction

[1.1] Ferene S as a sensitive iron(II) reagent	2
[1.2] Toxicity of mercury	2
[1.3] Mercury catalysis	5
[1.4] Stoichiometry of Ferene-iron Complex	6
[1.5] Chemical Kinetics	6
[1.5.1] The integrated rate method	7
[1.5.2] The Differential rate method	7
[1.6] Steady State Approximation	9
[1.7] Activation parameters & temperature effect	11
[1.7.1] Effect of temperature	11
[1.7.2] Transition state theory	11
[1.8] Kinetic methods of analysis	13
[1.8.1] The tangent method	13
[1.8.2] The fixed time method	13
[1.8.3] The fixed concentration method	13
[1.9] The purpose of this work	15

VII

Chapter Two: Experimental

[2.1] Chemicals	17
[2.2] Buffer Solutions	18
[2.3] Instrumentation	18
[2.4] Procedure	18
[2.5] Data Analysis procedure	19
[2.6] General procedure for mercury extraction and determination in medical samples	19

Chapter Three: Results and Discussion

[3.1] Absorption Spectra of the complex	22
[3.2] Effect of pH	23
[3.3] The catalyzed vs. the uncatalyzed reaction	27
[3.4] Effect of $K_4Fe(CN)_6$ Concentration	32
[3.5] Effect of Ferene Concentration	32
[3.6] Effect of $HgCl_2$ Concentration	41
[3.7] Effect of Temperature	44
[3.8] The reaction mechanism and rate law	55
[3.9] The rate constants	59
[3.10] Calibration graph	67
[3.11] Effect of Foreign ions	69
[3.12] Application	72
<i>References</i>	74

529523

VIII

List of Tables

<u>Table</u>	<u>Page</u>
1.1 A brief summary of the toxicity of mercury	4
3.1 Effect of pH on the complex formation	25
3.2 Time effect on absorbance of ferrous complex of Ferene S in the absence of HgCl_2 as catalyst.	28
3.3 Time effect on absorbance of ferrous complex of Ferene S in the presence of HgCl_2 as catalyst.	29
3.4 Effect of $\text{K}_4\text{Fe}(\text{CN})_6$ on the rate of complex formation in presence of HgCl_2 catalyst.	33
3.5 Effect of $\text{K}_4\text{Fe}(\text{CN})_6$ on the rate of complex formation in presence of HgCl_2 catalyst (at high $\text{K}_4\text{Fe}(\text{CN})_6$ concentrations)	34
3.6 Dependence of the rate on the concentration of Ferene S	37
3.7 Effect of Ferene S at higher concentration on the absorbance of the ferrous-Ferene complex.	38
3.8 Dependence of the rate on the concentration of HgCl_2	42
3.9 Effect of $\text{K}_4\text{Fe}(\text{CN})_6$ on the reaction rate of the reaction at different temperatures	45-46
3.10 Effect of temperature on the reaction rate	52
3.11 The activation parameters	54
3.12 The calculated rate constants	61

IX

<u>Table</u>	<u>Page</u>
3.13 The effect of lower concentrations of hexacyanoferrate(II) on the rate law	63
3.14 The effect of high concentrations of hexacyanoferrate(II) and Ferene on the rate law	65
3.15 The Calibration graph data	67
3.16 Effect of foreign cations and anions on the absorbance	70
3.17 Calculated mercury(II) content in a medicinal sample	64

List of Figures

<u>Figure</u>		<u>Page</u>
1.1	The tangents method	14
3.1	Absorption spectra of ferrous-Ferene complex	22
3.2	Effect of pH on the complex formation	26
3.3	Plot of absorbance vs. time for the uncatalyzed reaction	30
3.4	Plot of absorbance vs. time for the catalyzed reaction	31
3.5	Dependence of rate on the concentration of $K_4Fe(CN)_6$	35
3.6	Effect of $K_4Fe(CN)_6$ concentration on the absorbance	36
3.7	Dependence of rate on the concentration of Ferene	39
3.8	Effect of ligand concentration on the absorbance	40
3.9	Dependence of rate on the concentration of $HgCl_2$	43
3.10	Effect of temperature on the reaction rate at $15^\circ C$	47
3.11	Effect of temperature on the reaction rate at $25^\circ C$	48
3.12	Effect of temperature on the reaction rate at $30^\circ C$	49
3.13	Effect of temperature on the reaction rate at $40^\circ C$	50
3.14	Effect of temperature on the reaction rate at $50^\circ C$	51
3.15	A plot of $\ln k_{obs}$ versus $1/T$	53
3.16	A plot of Initial rate vs. $[K_4Fe(CN)_6]$	64

<u>Figure</u>	<u>Page</u>
3.17 A plot of Initial rate vs. $[\text{HgCl}_2]$ at high concentration of $[\text{K}_4\text{Fe}(\text{CN})_6]$ and Ferene	64
3.18 The calibration Curve for $[\text{Hg}^{2+}]$	68

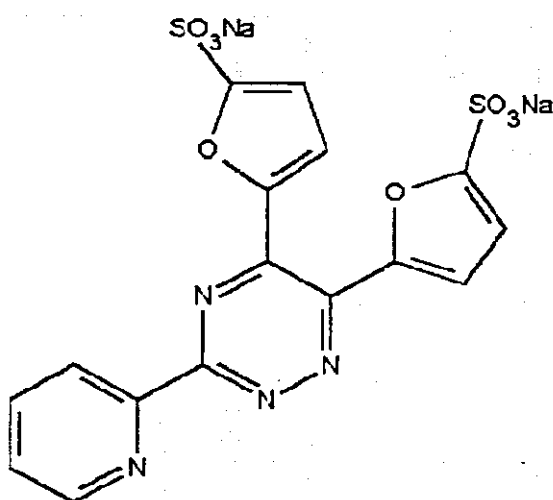
Chapter One

INTRODUCTION



[1.1] Ferene S as a sensitive iron(II) reagent:

Ferene (whose structure is shown below) is a highly sensitive iron reagent. This new reagent constitutes an alternative to the commonly used ferrozine for determination of serum iron ^[1-3].



Structure of Ferene S

[3 -(2-pyridyl)- 5,6-bis (2-(5- furyl sulfonic acid))- 1,2,4- triazine, disodium]

[1.2] Toxicity of mercury:

Mercury is known to be one of the most toxic substances in all of its chemical forms, as a metal, inorganic water-soluble salts, and organic salts.

Many research papers concerning the toxicity and determination of mercury as toxic element has been reported^[4-13].

The vapor pressure of metallic mercury is sufficiently high to cause acute mercury poisoning^[14-17]. On the other hand, some microorganisms can transform mercury compounds that present in water into methyl mercury (CH_3Hg^+), which concentrates in seafood and fish causing acute mercury poisoning^[14,18].

The main sources of inorganic mercury as toxic substances are wood preservatives, herbicides, insecticides, fireworks, batteries, thermometers, barometers, and in preparation of chlorine and sodium hydroxide. Organic mercury compounds are used as seed dressings, as fungicides, and in preventing mold^[18].

Mercury (II) chloride is a very toxic substance that causes acute kidney damage. Organic mercurials, especially methyl mercury (CH_3Hg^+), are more completely absorbed from the gastrointestinal tract. The short chain organic mercury compounds are usually distributed to the central nervous system (CNS) and are devoid of renal toxicity.

Table (1.1) gives a brief summary of the toxicity of mercury^[18]:

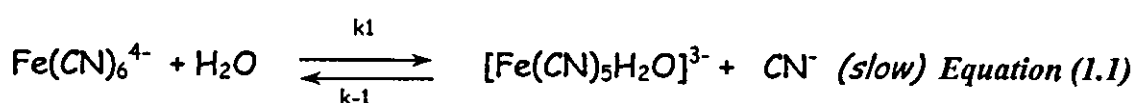
Table (1.1): A brief summary of the toxicity of mercury

Form Entering Body	Route of Absorption	Distribution	Target Organs for Toxicity	Metabolism	Elimination
<i>Elemental mercury</i>	Respiratory tract	CNS (where it is trapped as Hg^{2+}), Kidney (following conversion of the elemental Hg to Hg^{2+}).	CNS (Central Nervous System), Kidney (substantial due the conversion of the elemental Hg to Hg^{2+}).	The elemental Hg converted to Hg^{2+}	Urine (major) Feces (minor)
<i>Inorganic:</i> Hg^+ (less toxic) Hg^{2+} (more toxic)	Gastrointestinal, Skin (minor)	Kidney (predominant), blood, brain (minor)	Kidney, Gastrointestinal.	Hg^{2+} plus R-SH converted to Hg^+ -S-R, $Hg(S-R)_2$	Urine
<i>Organic:</i> alkyl, aryl, alkoxyalkyl	Gastrointestinal, Skin (substantial)	Kidney, brain, blood	CNS	R- Hg^{2+} converted to Hg^{2+} plus R (slow).	Urine

[1.3] Mercury catalysis:

Many workers have investigated the kinetics of abstraction of cyanide from hexacyanoferrate(II) by mercury(II) in the presence of many ligands in aqueous solutions such as ferrozine^[11,13,19], PAR^[13] (4-[pyridyl-(2)-azo]-resorcin-monosodium monohydrate), 2,2'-bipyridine^[20], *p*-NDA (*p*-nitrosodiphenylamine)^[21], nitrosobenzene^[22-26] and 2,4-bis(5,6-diphenyl-1,2,4-triazin-3-yl) pyridine tetrasulfonate (2,4-BDTPS)^[27].

The uncatalyzed reaction is an extremely slow process, where several days are needed to attain maximum absorbance. It is documented in the literature that the thermal decomposition of hexacyanoferrate(II) in the presence of water is a slow reversible process as shown below^[20-24, 26].



On the other hand, in the presence of a small amount of mercury the reaction proceeds at an appreciable rate and can be followed spectrophotometrically in short times, thus making feasible the determination of the toxic element mercury.

[1.4] Stoichiometry of Ferene-iron complex:

Iron(II) reacts with the ligand Ferene S (L^{2-}) to form a deep blue tris Ferene-iron(II) complex that absorbs at 593 nm^[2,3] according to:



The Stoichiometry of the complex was found by D. J. Hennessy and coworkers^[3], in which the molar-ratio and continuous variation methods confirm that Ferene behaves as bidentate chelating ligand forming the above *tris* Ferene-iron(II) complex.

[1.5] Chemical Kinetics:

It is convenient at this stage to discuss briefly general kinetic considerations and schemes. For the analysis of kinetic data two procedures are generally employed:

1) The integrated rate method

2) The differential rate method:

[1.5.1] The integrated rate method:

In this method integrated rate equations are used. For example for a first order reaction of the type:



the rate law is:

$$\text{Rate} = -\frac{d[A]}{dt} = k[A] \quad \text{Equation (1.3)}$$

Upon integration, this would lead to:

$$\ln([A]_0 / [A]_t) = kt \quad \text{Equation (1.4)}$$

In which A_t is the concentration at time equals t , A_0 is the concentration at time equals zero.

[1.5.2] The differential rate method:

In this work in employing differential rate method the concentration of all the reactants are kept in much excess over the substance (A) studied, thus isolating the latter, the initial rate method is used in conjunction with the isolation method. The rate is measured at the beginning of the reaction for several different initial concentrations of the reactants.

The rate law of the reaction, which is isolated, could be written as:

$$\text{Rate} = k [A]^n \quad \text{Equation(1.5)}$$

then the initial rate is given by the initial concentration of (A), that is :

$$\text{Initial rate} = k [A]^n_0 \quad \text{Equation(1.6)}$$

Upon taking logarithms for both sides the following equation is obtained:

$$\log(\text{initial rate}) = \log(k) + n \log[A]_0 \quad \text{Equation(1.7)}$$

where k is the rate constant, $[A]_0$ the initial molar concentration of A, and n is the order of the reaction.

This is an equation of a straight line, where a plot of $\log(\text{initial rate})$ versus $\log[A]_0$ will give a straight line of slope (n), which is the order of the reaction.

The advantage of this method over integration methods is that it does not depend on knowledge of the order of the reaction ^[29-34].

[1.6] The Steady State Approximation:

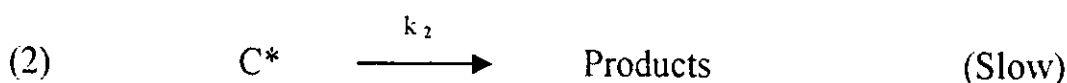
The steady state approximation is a technique that greatly simplifies the discussion of reaction schemes. It rests on the hypothesis that if a reaction intermediate (I^*) is formed then:

$$\frac{d[I^*]}{dt} = 0 \quad \text{Equation (1.8)}$$

this means:

the rate of the production of $[I^]$ = the rate of destruction of $[I^*]$*

To throw some light on this technique (which is used in this work) the following general reaction is considered:



In this scheme $[C^*]$ is considered as the reaction intermediate, applying steady state approximation we get:

529523

$$dC^*/dt = k_1 [A] [B] - k_{-1} [D] [C^*] - k_2 [C^*] = 0$$

$$\Rightarrow k_1 [A] [B] = k_{-1} [D] [C^*] + k_2 [C^*]$$

$$\Rightarrow k_1 [A] [B] = (k_{-1} [D] + k_2) [C^*]$$

$$[C^*] = \frac{k_1 [A] [B]}{k_{-1} [D] + k_2} \quad \text{Equation (1.9)}$$

The rate of the reaction is determined by the slow step (2) in the above reaction:

$$\text{Rate} = \frac{d[\text{Products}]}{dt} = k_2 [C^*] \quad \text{Equation(1.10)}$$

Substituting for $[C^*]$ in Equation (1.10) we have:

$$\text{Rate} = \frac{d[\text{Products}]}{dt} = k_2 \left[\frac{k_1 [A] [B]}{k_{-1} [D] + k_2} \right] \quad \text{Equation(1.11a)}$$

$$\text{Rate} = \frac{k_2 k_1 [A] [B]}{k_{-1} [D] + k_2} \quad \text{Equation(1.11b)}$$

Thus the general form of the rate law could be determined and correlated to the experimental rate law.

[1.7] Activation parameters & temperature effects

[1.7.1] Effect of temperature:

In general the rate of the reaction increases with increase in temperature. [34,35]. Arrhenius proposed the relation between the rate constant and temperature:

$$k_{obs} = A e^{-E^*/RT} \quad \text{Equation(1.12)}$$

A is called the frequency factor, or pre-exponential factor, E^* is the activation energy, R is the gas constant and T is the absolute temperature.

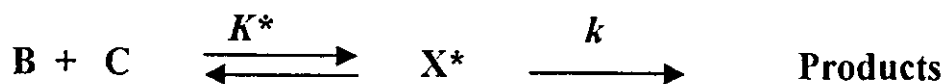
Upon taking the natural logarithm of Equation (1.12) we have:

$$\ln k_{obs} = \ln A - (E^*/RT) \quad \text{Equation(1.13)}$$

A plot of $\ln k_{obs}$ versus $1/T$, will give a straight line with slope of $-E^*/R$ and intercept of $\ln A$ from which E^* the energy of activation could be determined. The other thermodynamic parameters (ΔS^* , ΔH^* , ΔG^* , K^*) can be calculated using appropriate transition state theory equations [29-35]

[1.7.] Transition state theory:

The main idea is that the chemical reaction proceeds through a transition state for which an equilibrium exists between the reactants and the activated complex (X^*) for the reaction:



The rate constant is related to the free energy of activation (ΔG^*) by: ^[29,33]

$$k_r = \frac{RT}{N_A h} \exp(-\Delta G^*/RT) \quad \text{Equation(1.14)}$$

$$k_r = \frac{RT}{N_A h} \exp(\Delta S^*/R) \cdot \exp(-\Delta H^*/RT) \quad \text{Equation(1.15)}$$

E^* (the activation energy) is related to enthalpy of activation by:

$$\Delta H^* = E^* - nRT \quad \text{Equation(1.16)}$$

And $k_b = R/N_A$ Equation(1.17)

For solution reactions *Equation (1.15)* reduces to:

$$k_{obs} = \frac{k_b T}{h} \exp(1 + \Delta S^*/R) \cdot \exp(-E^*/RT) \quad \text{Equation(1.18)}$$

Comparing *Equation (1.18)* with Arrhenius *Equation (1.12)* we get: ^[29]

$$A = \frac{k_b T}{h} \exp(1 + \Delta S^*/R) \quad \text{Equation(1.19)}$$

Where

ΔH^* : The enthalpy of activation

ΔS^* : The entropy of activation

ΔG^* : The free energy of

k_b : The Boltzman constant.

activation

[1.8] Kinetic methods of analysis:

Kinetic methods of analysis using catalytic reactions are of extremely high sensitivity. It is possible to determine concentrations to an accuracy of 1×10^{-3} , 1×10^{-4} and even 1×10^{-6} of a microgram per milliliter.

Kinetic methods of analysis are definitely most useful for the determination of trace quantities of elements. They have been used successfully in determination of micro-quantities elements in biological samples.^[37]

Upon using kinetic methods of analysis, three sets of methods of determining concentration can be used:^[37]

(1.7.1) *The tangents method:*

In the differential modification of the tangents method the concentration of one of the substances being formed in definite time interval is measured and a graph of concentration of one of the substances being formed versus time is drawn up. The figure below (*Figure (1.1)*) explains this method:

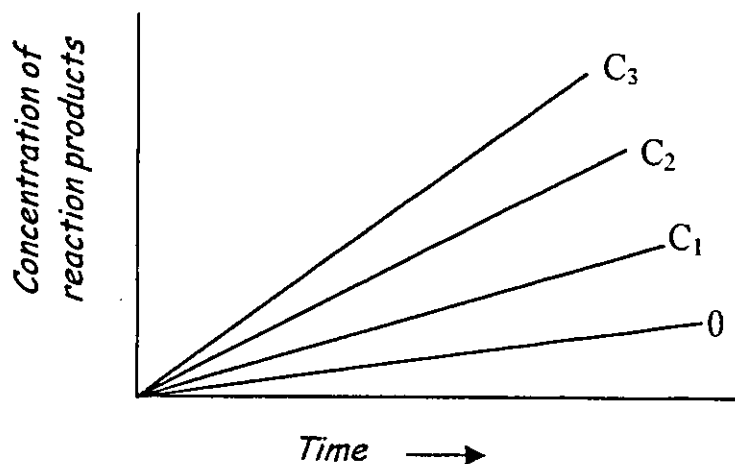


Figure (1.1): Dependence of concentration of reaction product on time at different concentrations of the substance being determined.

(1.7.2) The fixed time method:

In this method the reaction is allowed to proceed for a strictly determined time interval and after this time interval the concentration of one of the reactants in the solution is determined. This can be done by measuring some physico-chemical property of the solution at some specified instant or by stopping the reaction at a specified moment

(1.7.3) The fixed concentration method:

In using this method the time required for the concentration of one of the reactants to reach a specified value is measured

In this work the fixed time method is used in the analysis of data since this method proved to be reproducible giving good results.

[1.9] The purpose of this work

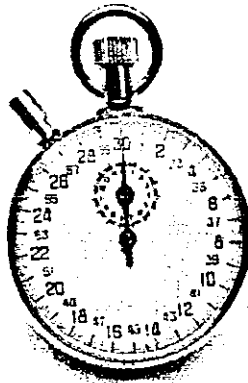
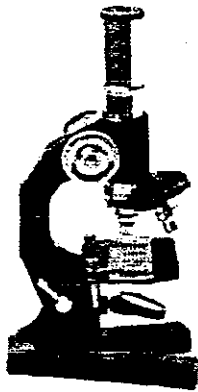
Pollution of plants and water with toxic mercury(II) salts is considered a dangerous matter because of its harmful effects on animals, plants, sea life and as well as human, so it is advantageous to look for a sensitive kinetic method for determination of mercury (II) in trace amount.

Hence the purpose of this work is to:

- I]. Study the kinetics and mechanism of the abstraction of cyanide from hexacyanoferrate(II) by the ligand Ferene S in the presence of mercury(II) as catalyst.
- II]. Proposing a new method for the determination of trace amounts of mercury in medicinal samples.

Chapter two

EXPERIMENTAL



[2.1] Chemicals:

Ferrocyanide solution:

A stock solution (1×10^{-2} M) of potassium hexacyanoferrate (II) trihydrate, ($\text{K}_4\text{Fe}(\text{CN})_6 \cdot 3\text{H}_2\text{O}$, M.wt. = 422.41 g/mole), was prepared daily using deionized water, and stored away from light and air by bubbling nitrogen into the solution and wrapping with aluminum foil^[20,21].

Ferene S solution:

Stock solution (1×10^{-2} M) of Ferene S, which is [3-(2-pyridyl)-5,6-bis (2-(5-furyl sulfonic acid))-1,2,4-triazine, disodium], (*Segma*), ($\text{C}_{16}\text{H}_8\text{N}_4\text{O}_8\text{S}_2\text{Na}_2$, M. wt = 494.4 g/mole) was prepared using deionized water.

Mercury (II) chloride solution:

Stock solution (1×10^{-2} M) of Mercury (II) Chloride, (*Aldrich*), (HgCl_2 , M. wt = 271.5 g/mole) was prepared in deionized water and kept in polyethylene bottle to prevent adsorption of the glass.

In each case, working solutions were prepared by appropriate dilution.

[2.2] Buffer solutions:

An array of buffer solutions were prepared in the pH range of (2.0-6.0) using acetic acid – sodium acetate and Hydrochloric acid – sodium acetate mixtures ^[38,39].

[2.3] Instrumentation:

UV/visible spectrophotometer:

The kinetics measurements were carried out using UV/visible spectrophotometer of the type (CPS-240A-UV/visible) with thermostatic attachments and two 1-cm glass cells.

pH meter:

The pH measurements were carried out using pH meter of type JENWAY 3310.

[2.4] Procedure:

Deionized water is used as solvent for all chemical preparations except for the buffer solutions, in which double distilled water was used.

Appropriate quantities of reactants were mixed in the following order: Ferene S, buffer, mercury(II)chloride, and $K_4Fe(CN)_6$. The solutions

were mixed inside 1-cm cell in a temperature controlled cell compartment using appropriate micropipettes. The zero time was taken at the moment of $K_4Fe(CN)_6$ addition. The reaction rates were followed by measuring the absorbance versus time at maximum wavelength of 593 nm, optimum pH = 3, and at temperature of $25.0 \pm 0.1^\circ C$, since this temperature is close to room temperature.

[2.5] Data Analysis Procedure:

Both pseudo first order kinetic plots and initial rate plots were used for the kinetic study.

Fixed time method was used for calibration curve sketching and mercury (II) content determinations.

[2.6] General procedure for mercury extraction and determination in medical samples:

Extraction:

Dissolve about (3-2 g) of Bleaching Cream that contains mercury salts in 5 ml of chloroform, shake well for 10 minutes. After the fatty cream has dissolved completely add about 3 ml of water, shake well for

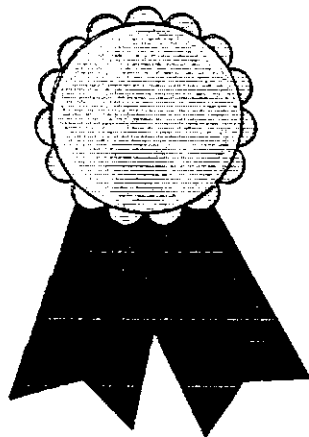
about 5 minutes. Allow the layers to separate. Centrifuge and decant the aqueous layer inside a 10-ml volumetric flask. Repeat water addition procedure twice. The combined water extracts were kept in a 10-ml volumetric flask and adjusted to volume.

Determination:

To 1 ml of $3.2 \times 10^{-3} M$ Ferene S mixed with 1 ml of acetate buffer (pH = 3), add 1 ml of mercury salt extract and 0.2 ml of $K_4Fe(CN)_6$ ($1.6 \times 10^{-3} M$). The absorbance was measured after 3 minutes at 593 nm against water blank as a reference solution. The time for the addition of $K_4Fe(CN)_6$ was taken as zero time.

Chapter three

RESULTS AND DISCUSSION



[3.1] Absorption Spectra of the complex:

The tris ferrous Ferene S complex absorbs at a maximum wavelength of *593 nm* as shown graphically in figure (3.1) below:

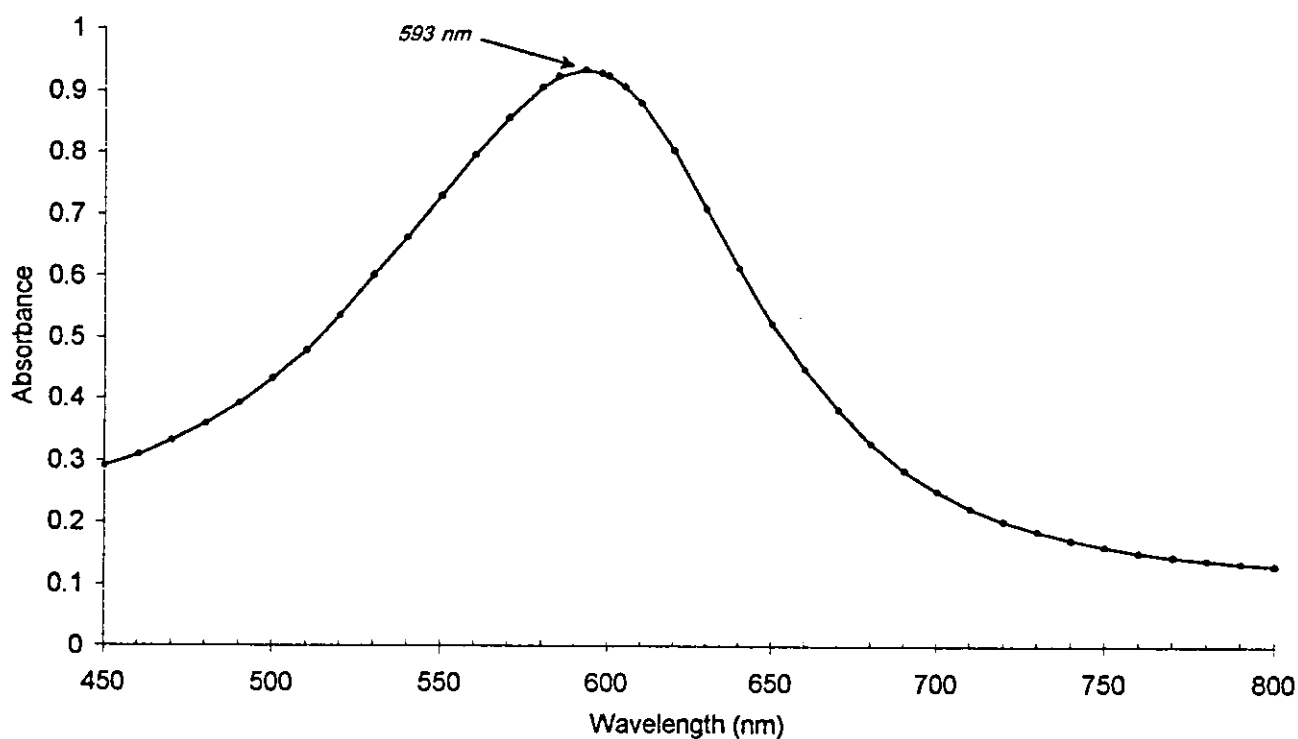


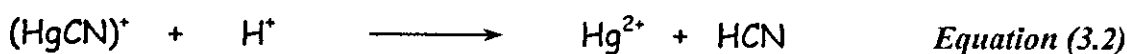
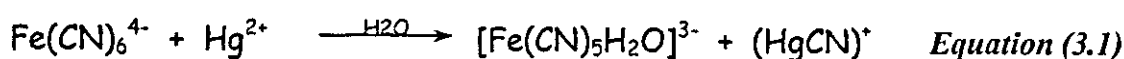
Figure (3.1): Absorption Spectra of the blue ferrous-Ferene Complex

[3.2] Effect of pH

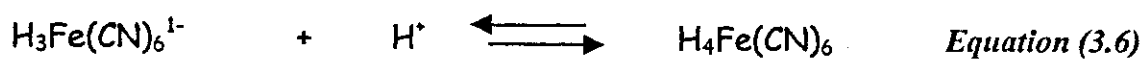
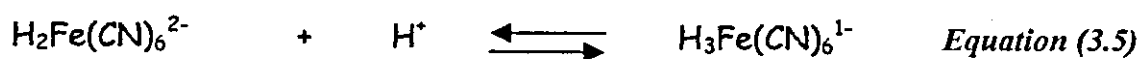
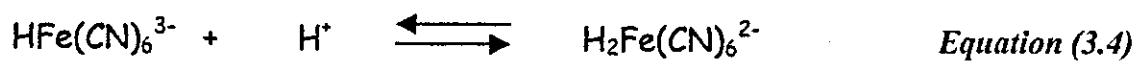
The effect of the pH on the absorbance of the ferrous complex was studied in the pH range (1.5 - 7) using acetate buffers. The data are tabulated in table (3.1) and shown graphically in figure (3.2).

As shown in below, the optimum pH was (3), therefore all our study and kinetic runs were made at this optimum pH of (3)

The rate of the reaction decrease at higher pH values. The decrease in the rate at higher pH values may be due to shortage of the protons needed to regenerate the catalytic species (*Equation (3.1) & Equation (3.2)*) and/or to the decrease in concentration of Hg^{2+} as a result of hydrolytic precipitation as hydroxide ^[13,25]



At low pH values the rate of the reaction is reduced probably due to the protonation of hexacyanoferrate(II) and/or protonation of the ligand is possible ^[21-25].



Where (L) in *Equations (3.7) and (3.8)*, symbolizes the ligand Ferene S.

Table (3.1): Effect of pH on the absorbance of the substitution of CN⁻ in hexacyanoferrate(II) by Ferene S at T = 25 °C using HgCl₂ as catalyst.

<i>pH</i>	<i>Absorbance</i> [*]
1.5	0.453
2	0.701
2.5	0.866
3	1.027
3.6	1.009
4.1	0.897
4.6	0.824
5.3	0.673
5.5	0.608
5.86	0.594
6.56	0.466

^{*} The absorbance was measured after 3 minutes

Conditions:

$[K_4Fe(CN)_6] = 1 \times 10^{-4} \text{ M}$

$pH = \text{varied (1.5-6.6)}$

$[Ferene \text{ S}] = 1 \times 10^{-3} \text{ M}$

$T = 25.0 \pm 0.1 \text{ } ^\circ\text{C}$

$[HgCl_2] = 1 \times 10^{-4} \text{ M}$

$\lambda_{\text{max}} = 593 \text{ nm}$

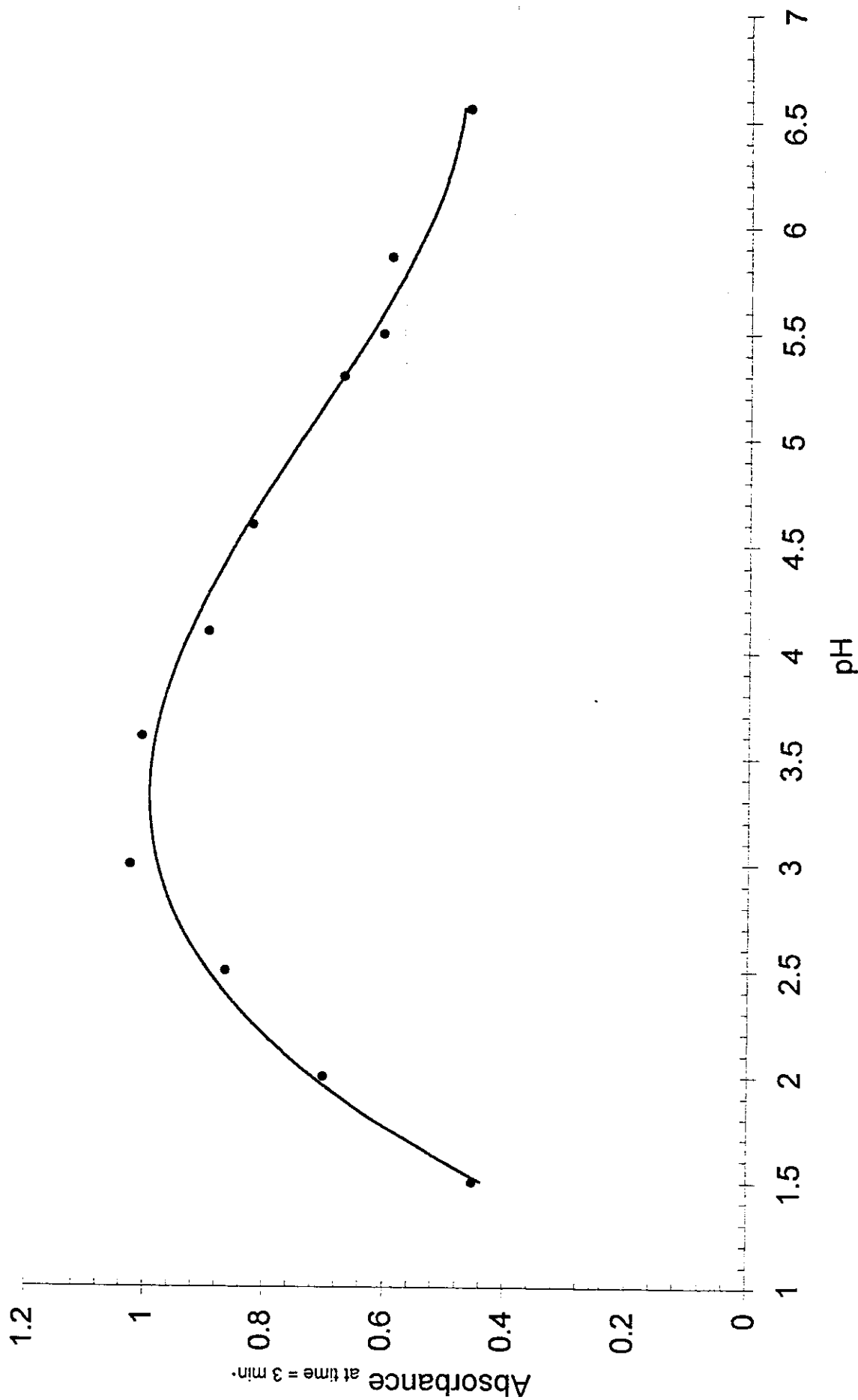


Figure (3.2): Effect of pH on the abstraction of cyanide from $K_4Fe(CN)_6$ in the presence of Ferene S.

$[Ferene] = 1 \times 10^{-3} M$, $[K_4Fe(CN)_6] = 1 \times 10^{-4} M$, $[HgCl_2] = 1 \times 10^{-4} M$, $T = 25^\circ C$

[3.3] The catalyzed vs. the uncatalyzed reaction:

The uncatalyzed reaction is an extremely slow process whereby it needs several days for completion. Whereas the catalyzed reaction in the presence of a trace amount of mercury (II) ($1 \times 10^{-4} M$) takes about 20 minutes for completion. This is presented graphically in Figures (3.3), (3.4) and tabulated in tables (3.2) and (3.3).

By carefully studying the tables it is seen clearly that for the catalyzed reaction the absorbance after *3 minutes* was *(0.6849)* while nearly it takes about *70 hours* to attain the same absorbance for the uncatalyzed reaction.

Table (3.2): Time effect on absorbance of ferrous-complex of Ferene S in the absence of HgCl_2 as catalyst.

Time*	Abs.	Time*	Abs.	Time*	Abs.	Time*	Abs.
0	0	17	0.2781	34	0.4241	51	0.5569
1	0.0333	18	0.2876	35	0.4323	52	0.5643
2	0.0599	19	0.2969	36	0.4407	53	0.5714
3	0.0869	20	0.3062	37	0.449	54	0.5785
4	0.1075	21	0.3149	38	0.4568	55	0.5857
5	0.127	22	0.3237	39	0.4647	56	0.593
6	0.1437	23	0.3325	40	0.4727	57	0.6003
7	0.1589	24	0.3412	41	0.4805	58	0.6077
8	0.1742	25	0.3499	42	0.4884	59	0.6149
9	0.1881	26	0.3584	43	0.4961	60	0.6221
10	0.2014	27	0.3667	44	0.5039	61	0.6288
11	0.2142	28	0.375	45	0.5116	62	0.635
12	0.226	29	0.3833	46	0.5192	63	0.6412
13	0.2373	30	0.3915	47	0.5269	64	0.6476
14	0.248	31	0.3998	48	0.5345	65	0.6527
15	0.2583	32	0.4078	49	0.542	65.5	0.6558
16	0.2684	33	0.4159	50	0.5498		

* Time in hours

Conditions

$$[\text{K}_4\text{Fe}(\text{CN})_6] = 1 \times 10^{-4} \text{ M}$$

$$T = 25.0 \pm 0.1 \text{ } ^\circ\text{C}$$

$$[\text{Ferene S}] = 1 \times 10^{-3} \text{ M}$$

$$\lambda_{\text{max}} = 593 \text{ nm}$$

$$\text{pH} = 3 \pm 0.1$$

Table (3.3): Time effect on absorbance of ferrous-complex of Ferene S in the presence of HgCl_2 as catalyst.

Time*	Abs.	Time*	Abs.	Time*	Abs.	Time*	Abs.
0	0.0248	15	2.223	30	2.6128	45	2.6587
1	0.2618	16	2.2802	31	2.6128	46	2.6587
2	0.4794	17	2.3457	32	2.6128	47	2.6587
3	0.6849	18	2.3823	33	2.6351	48	2.6587
4	0.8788	19	2.422	34	2.6351	49	2.6587
5	1.0597	20	2.4507	35	2.6351	50	2.6587
6	1.2283	21	2.4817	36	2.6351	51	2.6587
7	1.3835	22	2.4982	37	2.6351	52	2.6587
8	1.5276	23	2.5151	38	2.6351	53	2.6587
9	1.6851	24	2.5331	39	2.6587	54	2.6587
10	1.777	25	2.5518	40	2.6587	55	2.6587
11	1.8835	26	2.571	41	2.6587	56	2.6587
12	1.9843	27	2.571	42	2.6587	57	2.6587
13	2.0687	28	2.5914	43	2.6587	58	2.6587
14	2.1497	29	2.5914	44	2.6587	59	2.6587

* Time in minutes

Conditions

$$[\text{K}_4\text{Fe}(\text{CN})_6] = 1 \times 10^{-4} \text{ M}$$

$$[\text{Ferene S}] = 1 \times 10^{-3} \text{ M}$$

$$[\text{HgCl}_2] = 1 \times 10^{-4} \text{ M}$$

$$\text{pH} = 3 \pm 0.1$$

$$T = 25.0 \pm 0.1 \text{ } ^\circ\text{C}$$

$$\lambda_{\text{max}} = 593 \text{ nm}$$

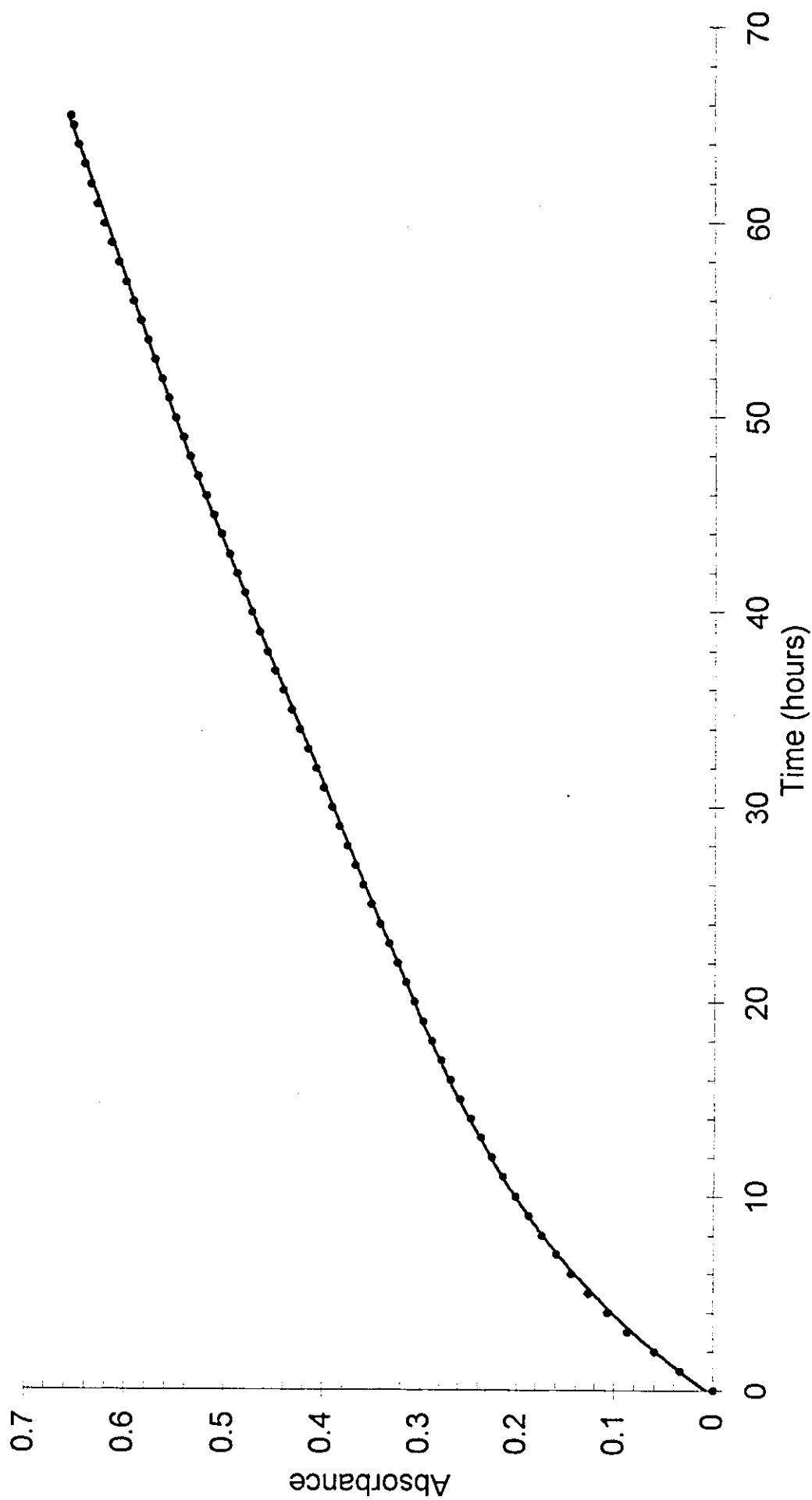


Fig (3.3): The plot of absorbance vs. time of the uncatalyzed reaction between Ferene S and $\text{K}_4\text{Fe}(\text{CN})_6$
 $[\text{K}_4\text{Fe}(\text{CN})_6] = 1 \times 10^{-4} \text{ M}$, $[\text{HgCl}_2] = 0 \text{ M}$, $[\text{Ferene}] = 1 \times 10^{-3} \text{ M}$, $T = 25^\circ \text{ C}$, $\text{pH} = 3$

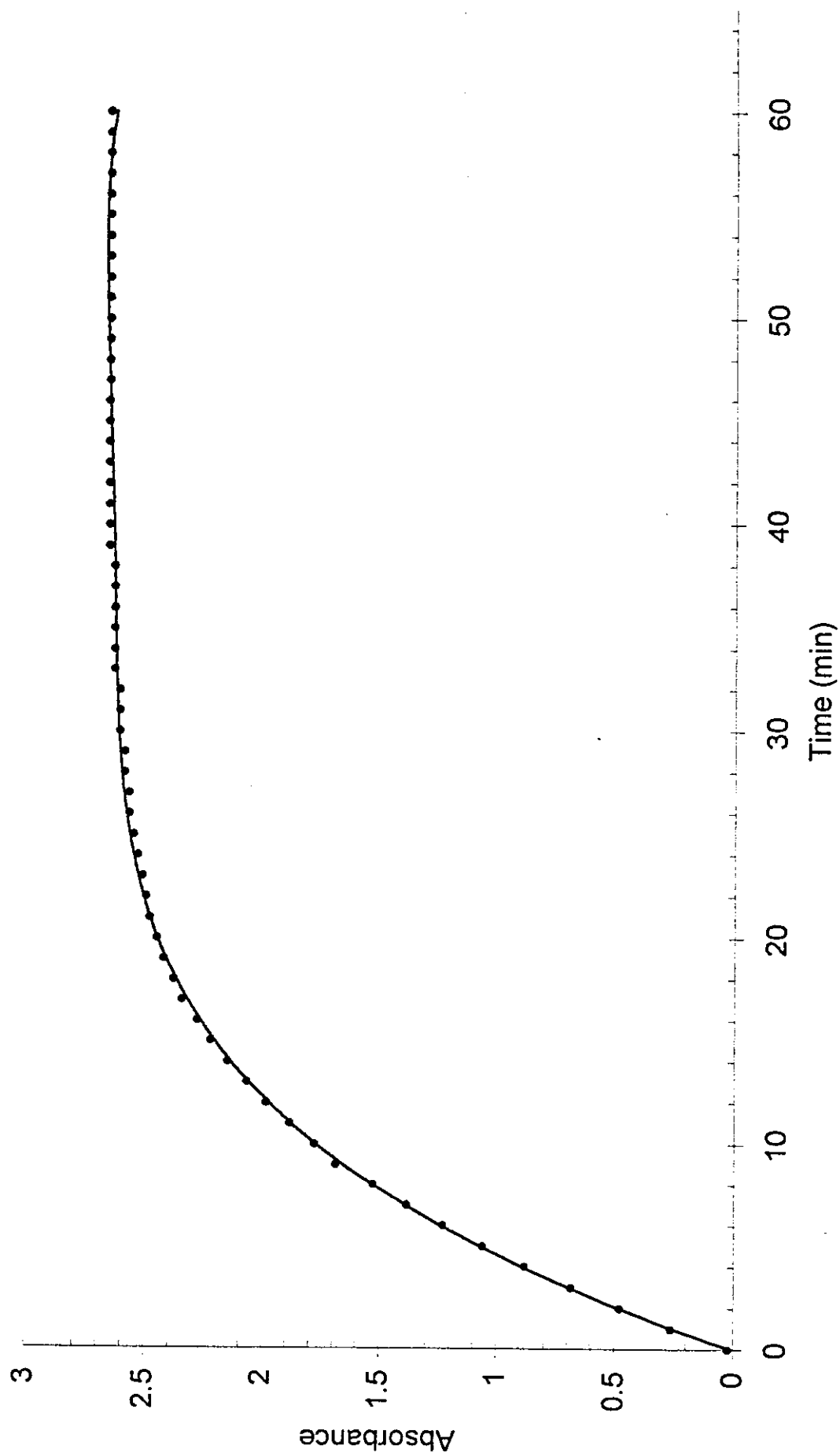


Fig (3.4): The plot of absorbance vs. time for the catalyzed reaction between Ferene S and $\text{K}_4\text{Fe}(\text{CN})_6$
 $[\text{K}_4\text{Fe}(\text{CN})_6] = 1 \times 10^{-4} \text{ M}$, $[\text{HgCl}_2] = 1 \times 10^{-4} \text{ M}$, $[\text{Ferene}] = 1 \times 10^{-3} \text{ M}$, $T = 25^\circ \text{ C}$, $\text{pH} = 3$

[3.4] Effect of $K_4Fe(CN)_6$ Concentration

It was found that the order of the reaction was unity at low concentrations of potassium hexacyanoferrate(II) as shown graphically in figure (3.5) and presented in table (3.4).

It was observed also that the order with respect to potassium hexacyanoferrate(II) tends to zero at high potassium hexacyanoferrate(II) concentrations. This is clearly apparent in figure (3.6) and table (3.5)

[3.5] Effect of Ferene Concentration

The effect of the ligand Ferene S is shown in table (3.6), and presented in figure (3.7). A straight line with a slope of unity was obtained upon plotting $\log(\text{initial rate})$ versus $\log[\text{Ferene S}]$, figure (3.7), indicating the rate is first order with respect to Ferene S.

At high Ferene concentrations the absorbance after 3 minutes was nearly constant indicating zero order with respect to Ferene S. This is presented in table (3.7) and shown graphically in figure (3.8)

Table (3.4): The effect of potassium hexacyanoferrate(II) on the rate of the formation of Ferene S-iron(II) complex in the presence of HgCl_2 catalyst

$[\text{K}_4\text{Fe}(\text{CN})_6]$ <i>M</i>	Initial rate (min^{-1})	$\log[\text{K}_4\text{Fe}(\text{CN})_6]$	$\text{Log}(\text{initial rate})$
7×10^{-6}	0.0328	-5.1549	-1.48479
8×10^{-6}	0.039	-5.0969	-1.40949
9×10^{-6}	0.0468	-5.0458	-1.32975
1×10^{-5}	0.0489	-5.0	-1.31069
2×10^{-5}	0.0936	-4.699	-1.02896
3×10^{-5}	0.136	-4.5229	-0.86646
4×10^{-5}	0.2206	-4.3979	-0.65639
5×10^{-5}	0.3023	-4.3010	-0.51963
6×10^{-5}	0.3149	-4.2218	-0.50183

Conditions

$$[\text{Ferene S}] = 1 \times 10^{-3} \text{ M}$$

$$T = 25.0 \pm 0.1 \text{ } ^\circ\text{C}$$

$$[\text{HgCl}_2] = 1 \times 10^{-4} \text{ M}$$

$$\lambda_{\text{max}} = 593 \text{ nm}$$

$$\text{pH} = 3 \pm 0.1$$

Table (3.5): The effect of potassium hexacyanoferrate(II) on the absorbance of ferrous-Ferene S complex in the presence of HgCl₂ catalyst

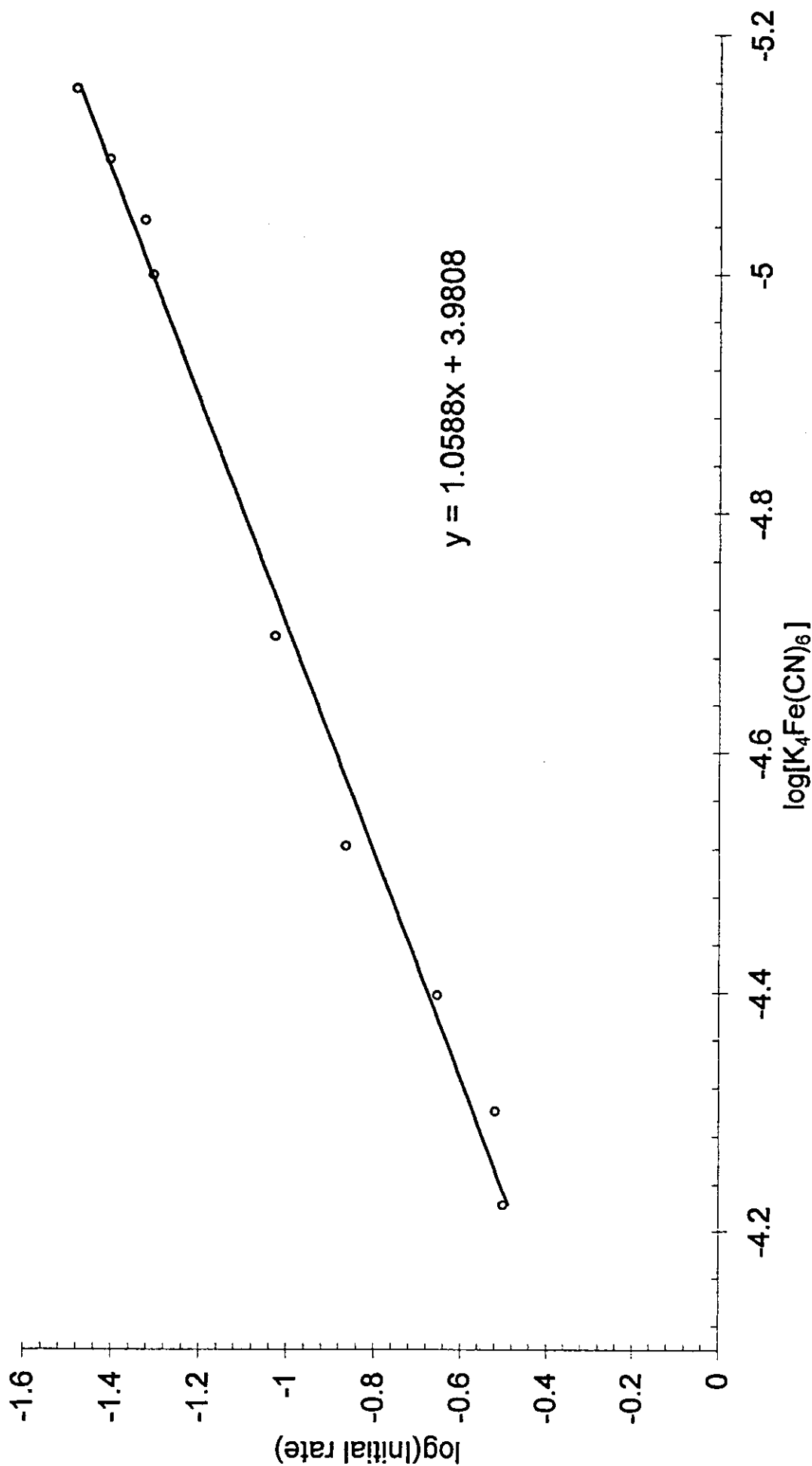
$[K_4Fe(CN)_6]$ <i>M</i>	Absorbance*	$[K_4Fe(CN)_6]$ <i>M</i>	Absorbance*
7×10^{-6}	0.1464	6×10^{-5}	1.1322
8×10^{-6}	0.1655	7×10^{-5}	1.1601
9×10^{-6}	0.1853	8×10^{-5}	1.1956
1×10^{-5}	0.1948	1×10^{-4}	1.2521
2×10^{-5}	0.3337	1.2×10^{-4}	1.2433
3×10^{-5}	0.4658	1.5×10^{-4}	1.2363
4×10^{-5}	0.6759	1.7×10^{-4}	1.2247
5×10^{-5}	0.9246	2×10^{-4}	1.2196

* The absorbance was measured after 3 minutes

Conditions

[Ferene S] = 1×10^{-3} M
[HgCl₂] = 1×10^{-4} M
pH = 3 ± 0.1

T = 25.0 ± 0.1 °C
 λ_{max} = 593 nm



Fig(3.5): A plot of $\log(\text{initial rate})$ vs. $\log[\text{K}_4\text{Fe}(\text{CN})_6]$
[HgCl_2] = 1×10^{-4} M, [Ferene] = 1×10^{-3} M, T = 25 ° C, pH = 3

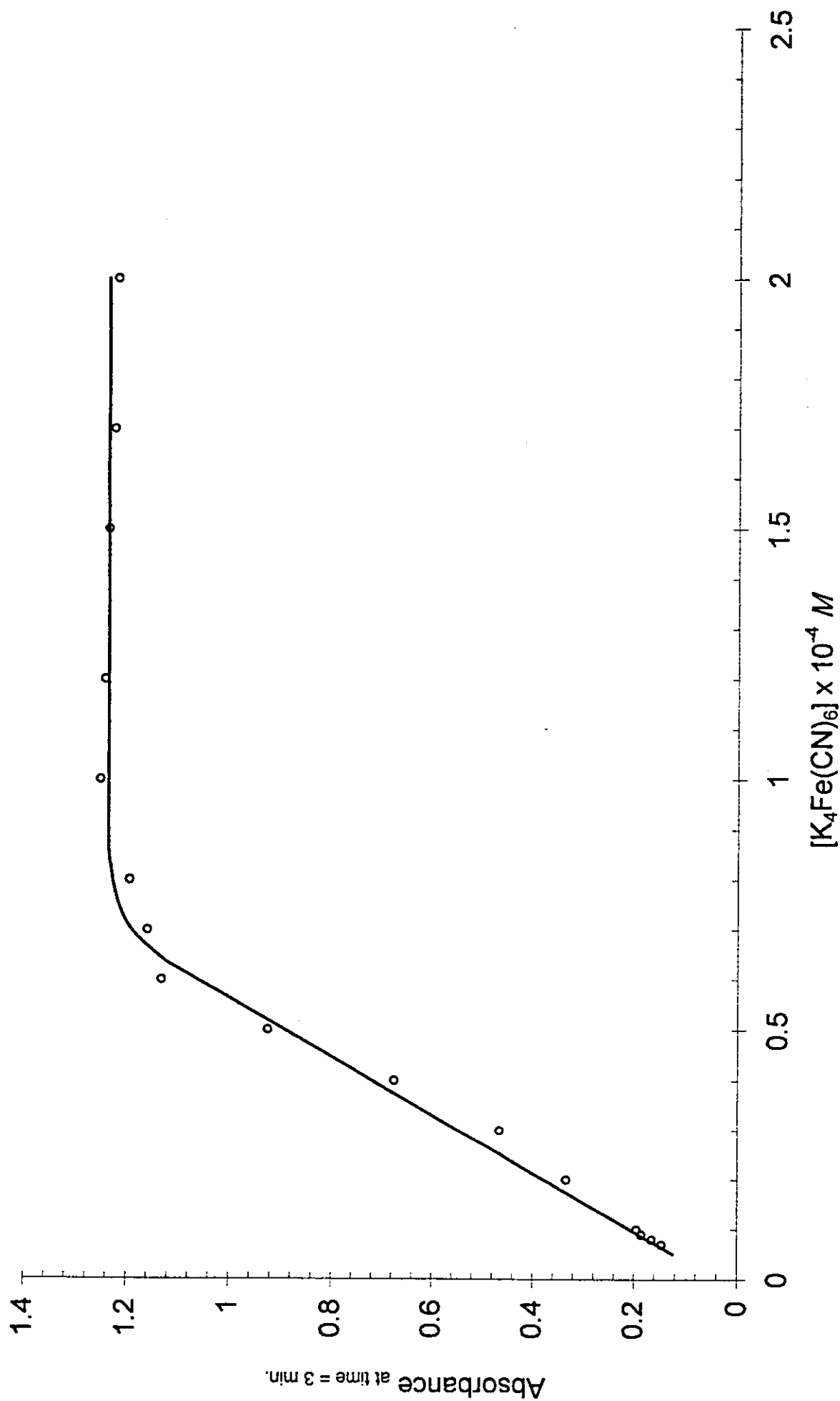


Figure (3.6): Effect of $K_4Fe(CN)_6$ concentration on the absorbance in presence of Ferene S

$[Ferene\ S] = 1 \times 10^{-3} M$, $[HgCl_2] = 1 \times 10^{-4} M$, $T = 25^\circ C$, $pH = 3$

Table (3.6): The effect of Ferene S on the rate of the Ferene-iron(II) complex formation in the presence of HgCl_2 as catalyst.

[Ferene S] <i>M</i>	Initial rate (<i>min</i> ⁻¹)	log[Ferene S]	Log(initial rate)
2×10^{-5}	0.0163	-4.69897	-1.78781
3×10^{-5}	0.0256	-4.522879	-1.59176
4×10^{-5}	0.04255	-4.39794	-1.3711
5×10^{-5}	0.0605	-4.30103	-1.21824
6×10^{-5}	0.06775	-4.221849	-1.16909
7×10^{-5}	0.0877	-4.154902	-1.057
8×10^{-5}	0.0912	-4.09691	-1.04001
9×10^{-5}	0.1058	-4.045757	-0.97551
1×10^{-4}	0.1095	-4	-0.96059

Conditions

$$[\text{K}_4\text{Fe}(\text{CN})_6] = 1 \times 10^{-4} \text{ M}$$

$$T = 25.0 \pm 0.1 \text{ } ^\circ\text{C}$$

$$[\text{HgCl}_2] = 1 \times 10^{-4} \text{ M}$$

$$\lambda_{\text{max}} = 593 \text{ nm}$$

$$\text{pH} = 3 \pm 0.1$$

Table (3.7): The effect of Ferene S on the absorbance of the ferrous-Ferene complex in the presence of HgCl_2 as catalyst.

[Ferene S] <i>M</i>	<i>Absorbance*</i>	[Ferene S] <i>M</i>	<i>Absorbance*</i>
2×10^{-5}	0.0562	1.5×10^{-4}	0.9661
3×10^{-5}	0.097	2×10^{-4}	1.1595
4×10^{-5}	0.1647	3×10^{-4}	1.2001
5×10^{-5}	0.1973	5×10^{-4}	1.2051
6×10^{-5}	0.3086	7×10^{-4}	1.2103
7×10^{-5}	0.3967	1×10^{-3}	1.1581
8×10^{-5}	0.4766	1.2×10^{-3}	1.1972
9×10^{-5}	0.5677	1.5×10^{-3}	1.176
1×10^{-4}	0.6343		

* The absorbance was measured after 3 minutes

Conditions

$$[\text{K}_4\text{Fe}(\text{CN})_6] = 1 \times 10^{-4} \text{ M}$$

$$[\text{HgCl}_2] = 1 \times 10^{-4} \text{ M}$$

$$\text{pH} = 3 \pm 0.1$$

$$T = 25.0 \pm 0.1 \text{ } ^\circ\text{C}$$

$$\lambda_{\text{max}} = 593 \text{ nm}$$

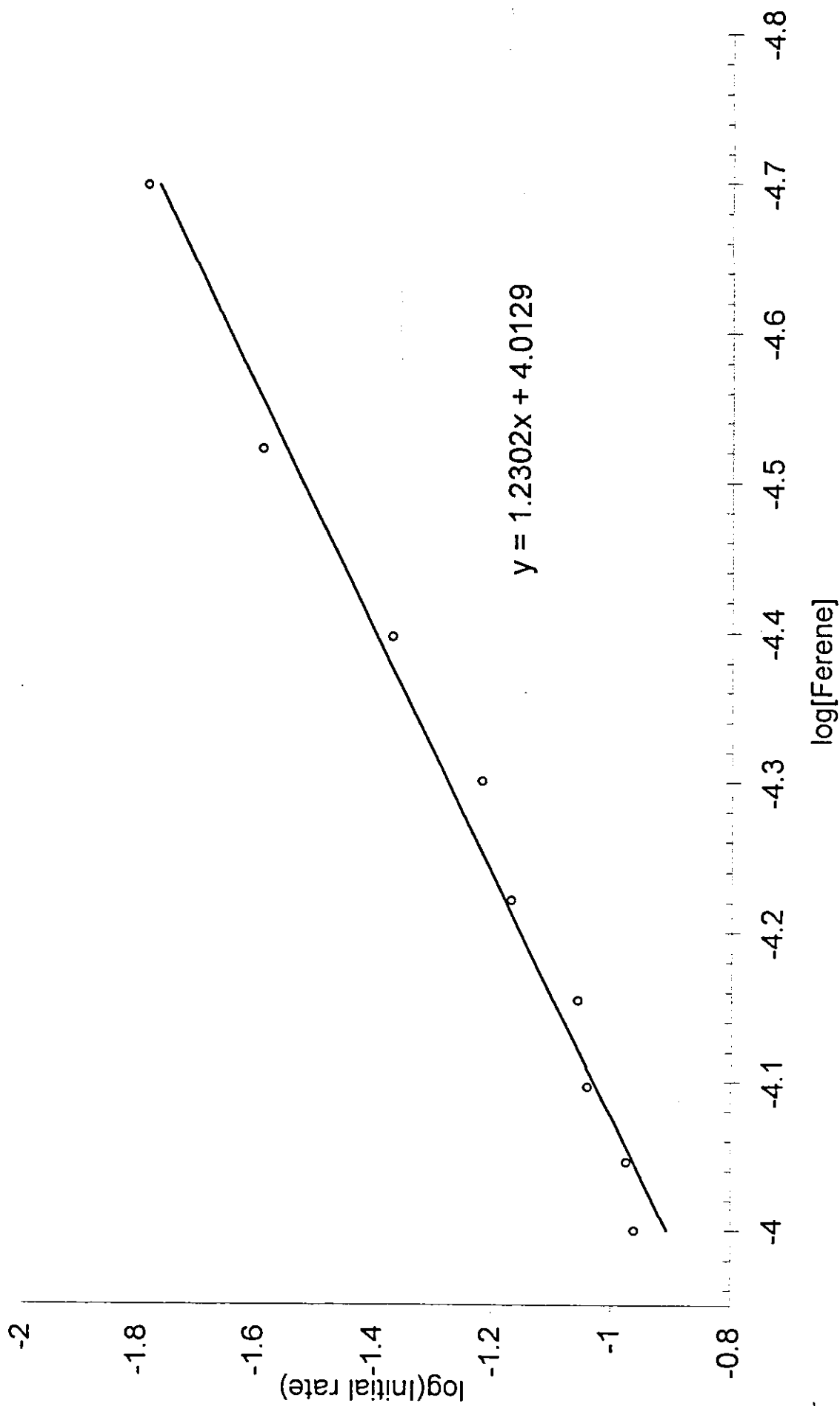


Figure (3.7): Effect of ligand, a plot of $\log(\text{initial rate})$ vs. $\log[\text{Ferene S}]$
 $[\text{K}_4\text{Fe}(\text{CN})_6] = 1 \times 10^{-4} \text{ M}$, $[\text{HgCl}_2] = 1 \times 10^{-4} \text{ M}$, $\text{pH} = 3$, $T = 25^\circ \text{ C}$

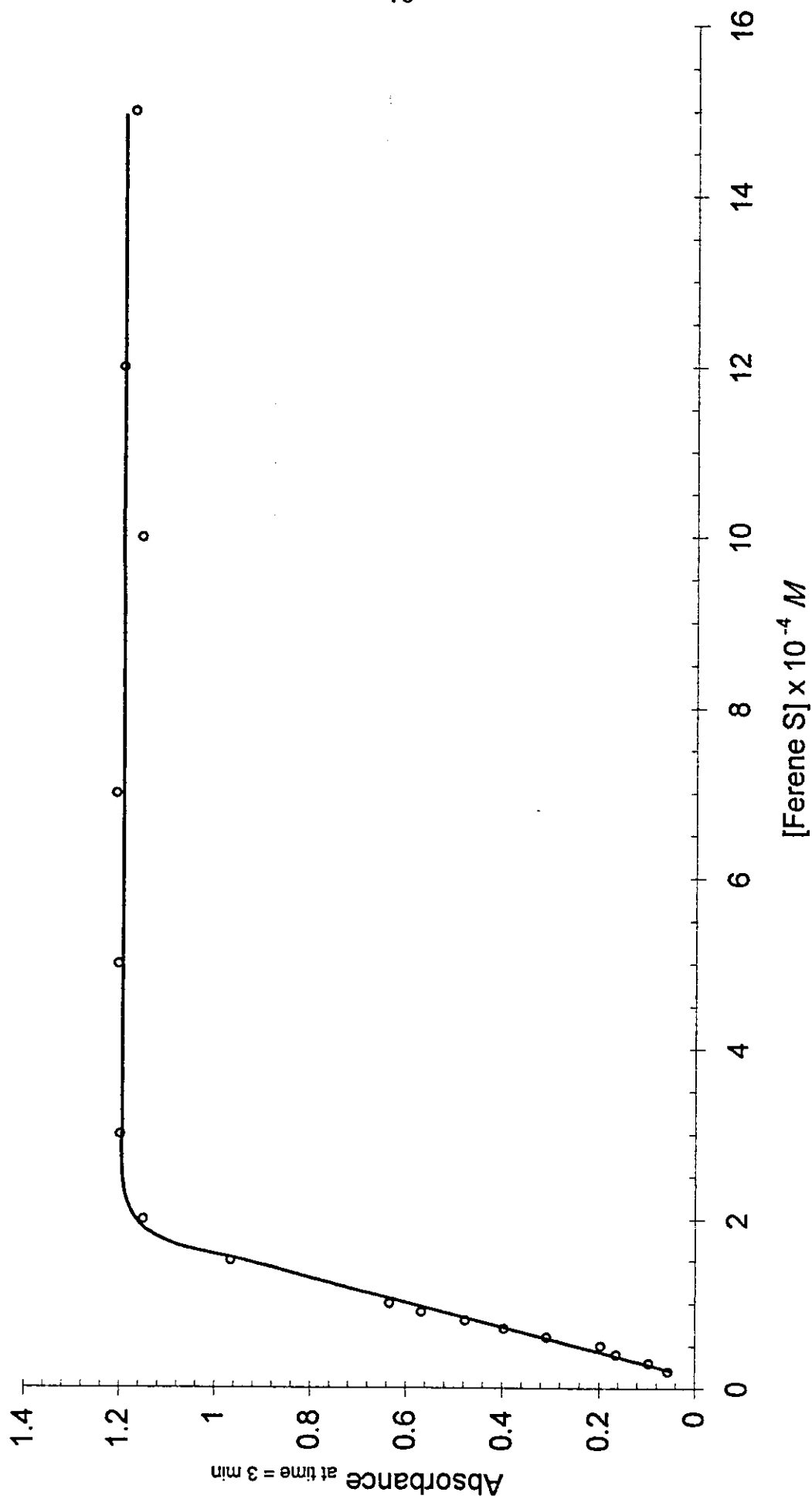


Figure (3.8): Effect of ligand concentration, a plot of Absorbance vs. $[\text{Ferene S}]$

$[\text{K}_4\text{Fe}(\text{CN})_6] = 1 \times 10^{-4} \text{ M}$, $[\text{HgCl}_2] = 1 \times 10^{-4} \text{ M}$, $\text{pH} = 3$, $T = 25^\circ \text{C}$

[3.6] Effect of HgCl_2 Concentration

The effect of $[\text{HgCl}_2]$ on the absorbance of the blue complex was studied with $[\text{Ferene}] = 1 \times 10^{-3} \text{ M}$ and $[\text{K}_4\text{Fe}(\text{CN})_6] = 1 \times 10^{-4} \text{ M}$, $\text{pH} = 3$, and temperature of 25° C . A straight line was obtained by plotting \log (initial rate) vs. $\log[\text{HgCl}_2]$ with slope of unity, indicating that the effect of $[\text{HgCl}_2]$ follows first order plot.

The results are represented in table (3.8), and shown graphically in Figure (3.9).

Table (3.8): The effect of mercury(II) chloride on the rate of the Ferene-iron(II) complex formation.

Initial Rate	[HgCl ₂]	log Initial Rate	log [HgCl ₂]
0.0008	7×10^{-7}	-3.09691	-6.154902
0.0011	1×10^{-6}	-2.95861	-6
0.00245	2×10^{-6}	-2.61083	-5.69897
0.00395	3×10^{-6}	-2.4034	-5.522879
0.0054	4×10^{-6}	-2.26761	-5.39794
0.0073	5×10^{-6}	-2.13668	-5.30103
0.0094	6×10^{-6}	-2.02687	-5.221849
0.01135	7×10^{-6}	-1.945	-5.154902
0.01435	8×10^{-6}	-1.84315	-5.09691
0.01315	9×10^{-6}	-1.88107	-5.045757
0.0163	1×10^{-5}	-1.78781	-5

Conditions :

$$[\text{K}_4\text{Fe}(\text{CN})_6] = 1 \times 10^{-4} \text{ M}$$

$$T = 25.0 \pm 0.1 \text{ } ^\circ\text{C}$$

$$[\text{Ferene S}] = 1 \times 10^{-3} \text{ M}$$

$$\lambda_{\text{max}} = 593 \text{ nm}$$

$$\text{pH} = 3 \pm 0.1$$

529523

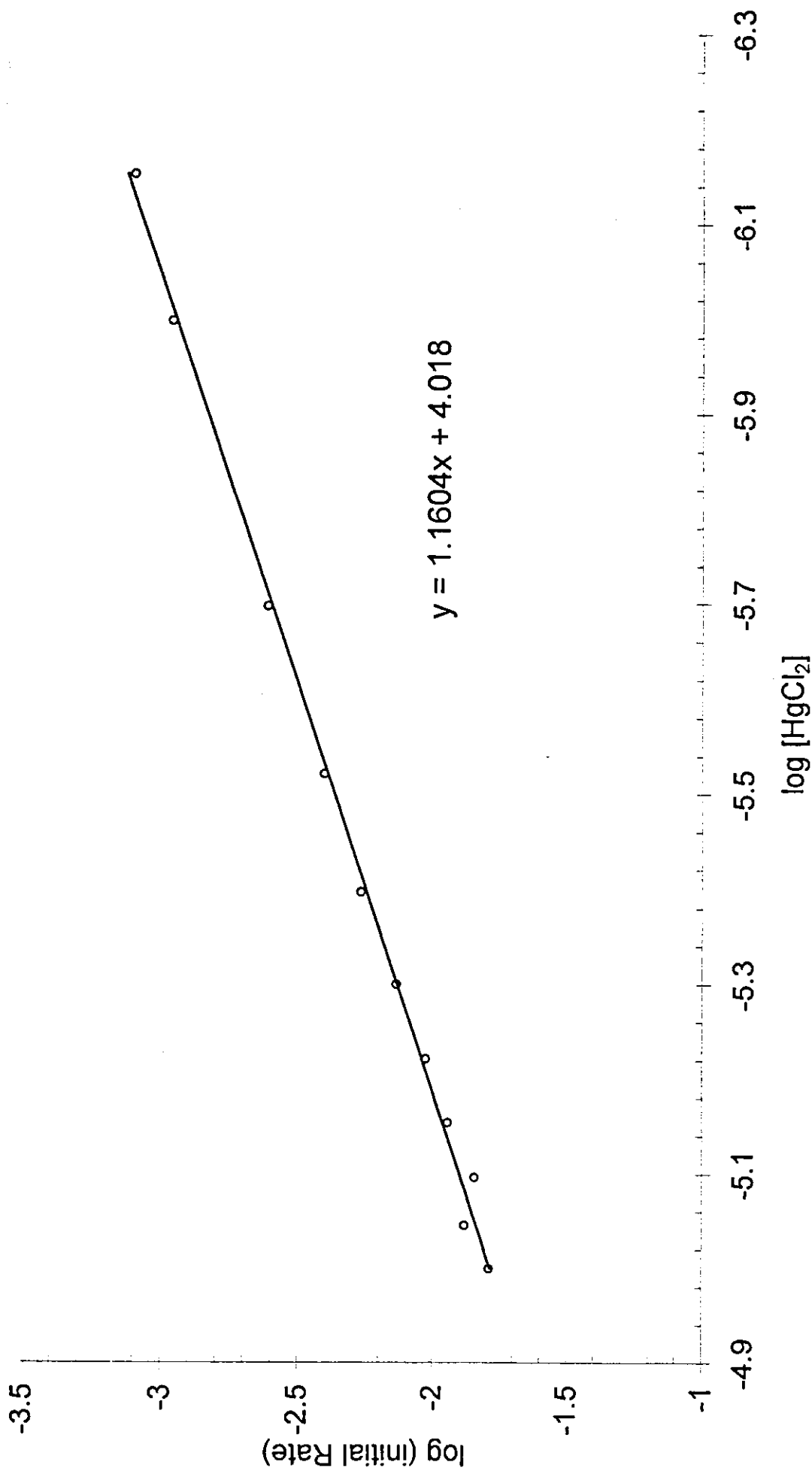


Fig (3.9): A plot of log(initial rate) vs. log [HgCl₂] in the presence of Ferene S.
 [K₄Fe(CN)₆] = 1 × 10⁻⁴ M, [Ferene] = 1 × 10⁻³ M, pH = 3, T = 25° C.

[3.7] Effect of Temperature

The effect of temperature on the absorbance of the complex was studied in the temperature range 15-50 °C. Plots of Initial rate versus different concentrations of $[K_4Fe(CN)_6]$ at different temperatures gave straight lines with different slopes each one equals to k_{obs} at that temperature . Table (3.9) and figures (3.10) - (3.14) illustrate all.

Upon plotting $\ln k_{obs}$ versus $1/T$, as indicated in Arrhenius equation a straight line was obtained. From the slope of this line the activation energy can be calculated. The data is depicted in table (3.10) and figure (3.15).

Using appropriate transition state theory equations, activation parameters were determined and tabulated in table (3.11)

Table (3.9): The effect of potassium hexacyanoferrate(II) on the rate of the formation of Ferene S-iron(II) complex in the presence of HgCl_2 catalyst at various temperatures.

Temperature °C	$[\text{K}_4\text{Fe}(\text{CN})_6]$ <i>M</i>	Initial rate (min^{-1})	$[\text{K}_4\text{Fe}(\text{CN})_6]$ <i>M</i>	Initial rate (min^{-1})
15 °C	0.000001	0.00057	0.000007	0.00557
	0.000003	0.00193	0.000009	0.006
	0.000005	0.00283	0.000011	0.00773
25 °C	0.000001	0.00243	0.000007	0.01737
	0.000003	0.00703	0.000009	0.0238
	0.000005	0.01187	0.000011	0.02853
30 °C	0.000001	0.0038	0.000007	0.0372
	0.000003	0.0125	0.000009	0.04003
	0.000005	0.02047	0.000013	0.06447
40 °C	0.000001	0.00697	0.000007	0.0611
	0.000003	0.02227	0.000009	0.07633
	0.000005	0.04287	0.000011	0.10783

Temperature °C	$[\text{K}_4\text{Fe}(\text{CN})_6]$ <i>M</i>	Initial rate (<i>min</i> ⁻¹)	$[\text{K}_4\text{Fe}(\text{CN})_6]$ <i>M</i>	Initial rate (<i>min</i> ⁻¹)
50 °C	0.000001	0.0087	0.000007	0.07363
	0.000003	0.02947	0.000009	0.09703
	0.000005	0.05307	0.000011	0.11883

Conditions

$[\text{Ferene S}] = 0.8 \times 10^{-3} \text{ M}$

$[\text{HgCl}_2] = 0.8 \times 10^{-4} \text{ M}$

$[\text{KNO}_3] = 0.1 \text{ M}$

$\text{pH} = 3 \pm 0.1$

$\lambda_{\text{max}} = 593 \text{ nm}$

$T = 15\text{-}50.0 \pm 0.1 \text{ }^\circ\text{C}$

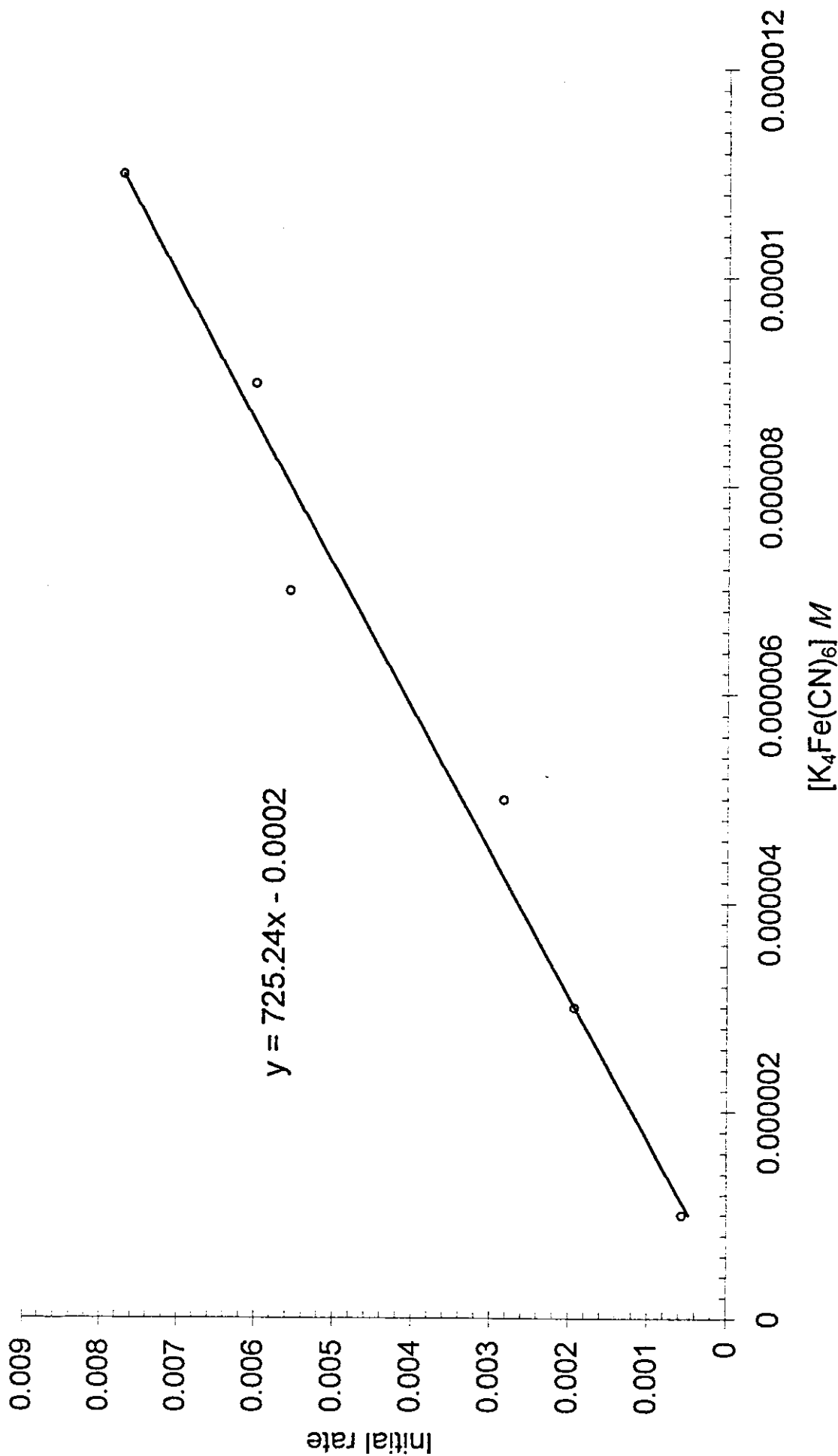


Figure (3.10): A plot of Initial rate vs. [K₄Fe(CN)₆]
[Ferene] = 0.8x10⁻³ M, [HgCl₂] = 0.8x10⁻⁴ M, [KNO₃] = 0.1 M, T = 15 ° C, pH = 3

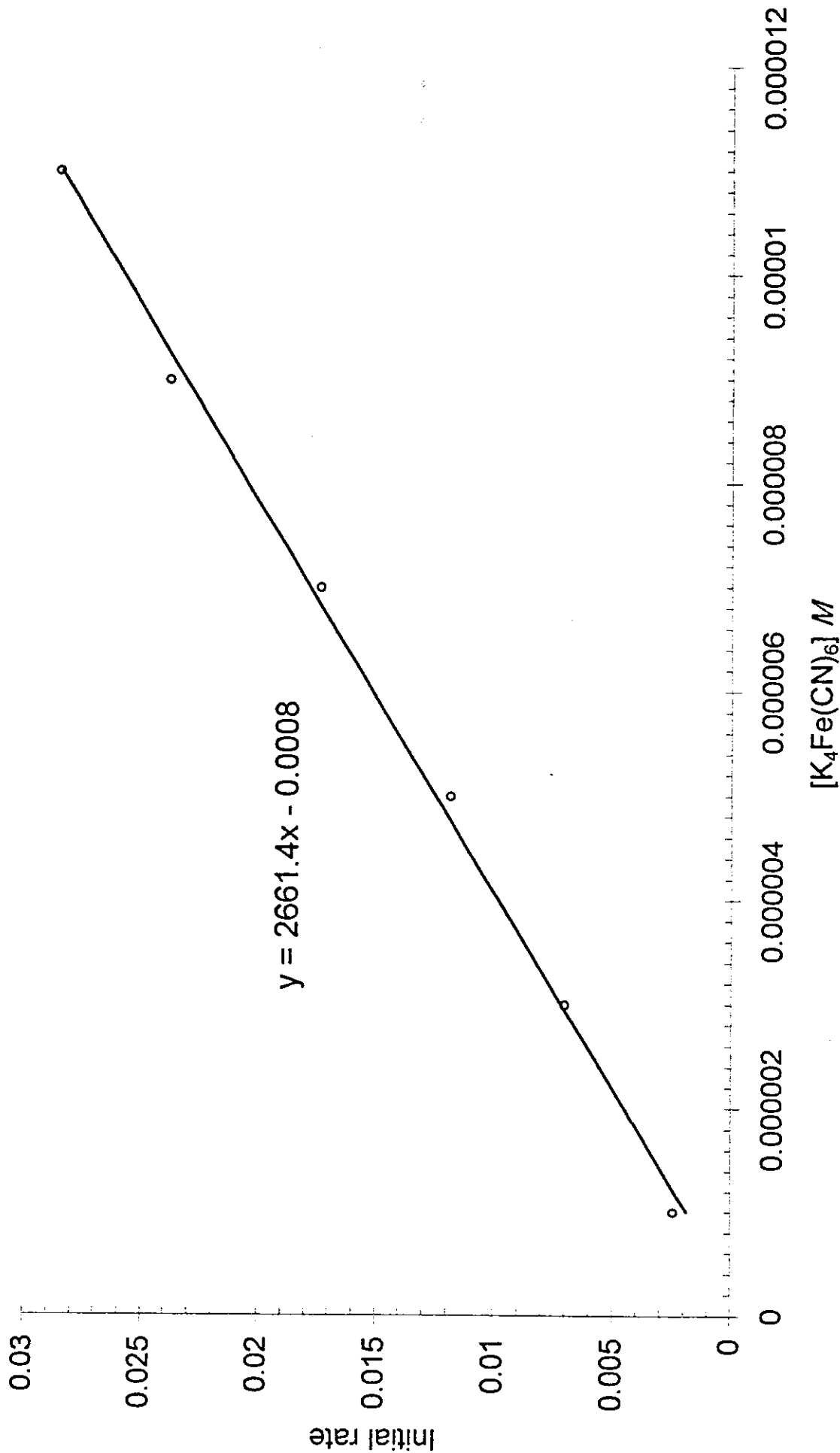


Figure (3.11): A plot of Initial rate vs. $[K_4Fe(CN)_6]$

$[Ferene] = 0.8 \times 10^{-3} M$, $[HgCl_2] = 0.8 \times 10^{-4} M$, $[KNO_3] = 0.1 M$, $T = 25^\circ C$, $pH = 3$

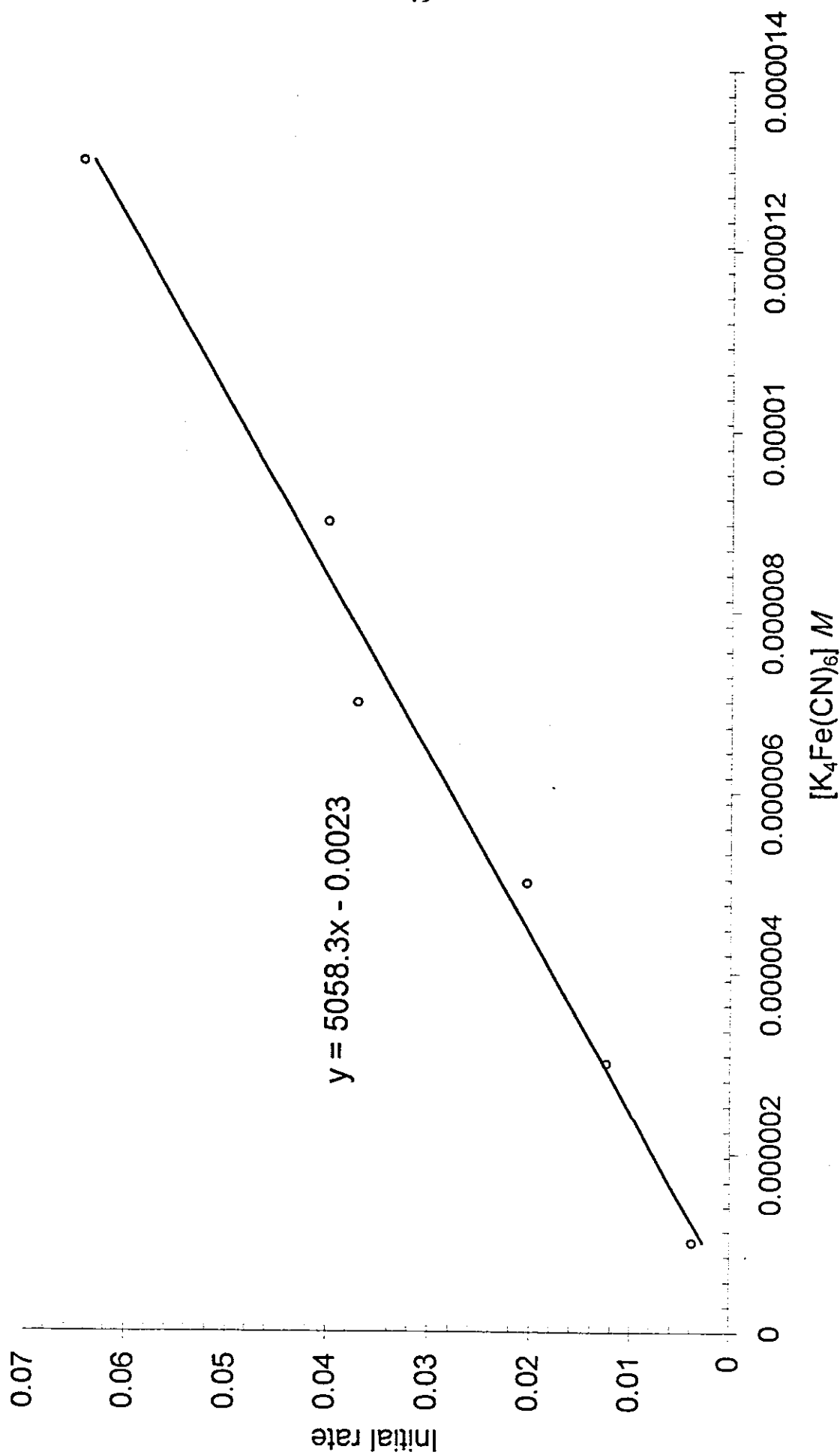


Figure (3.12): A plot of Initial rate vs. $[K_4Fe(CN)_6]$

$[Ferene] = 0.8 \times 10^{-3} M$, $[HgCl_2] = 0.8 \times 10^{-4} M$, $[KNO_3] = 0.1 M$, $T = 30^\circ C$, $pH = 3$

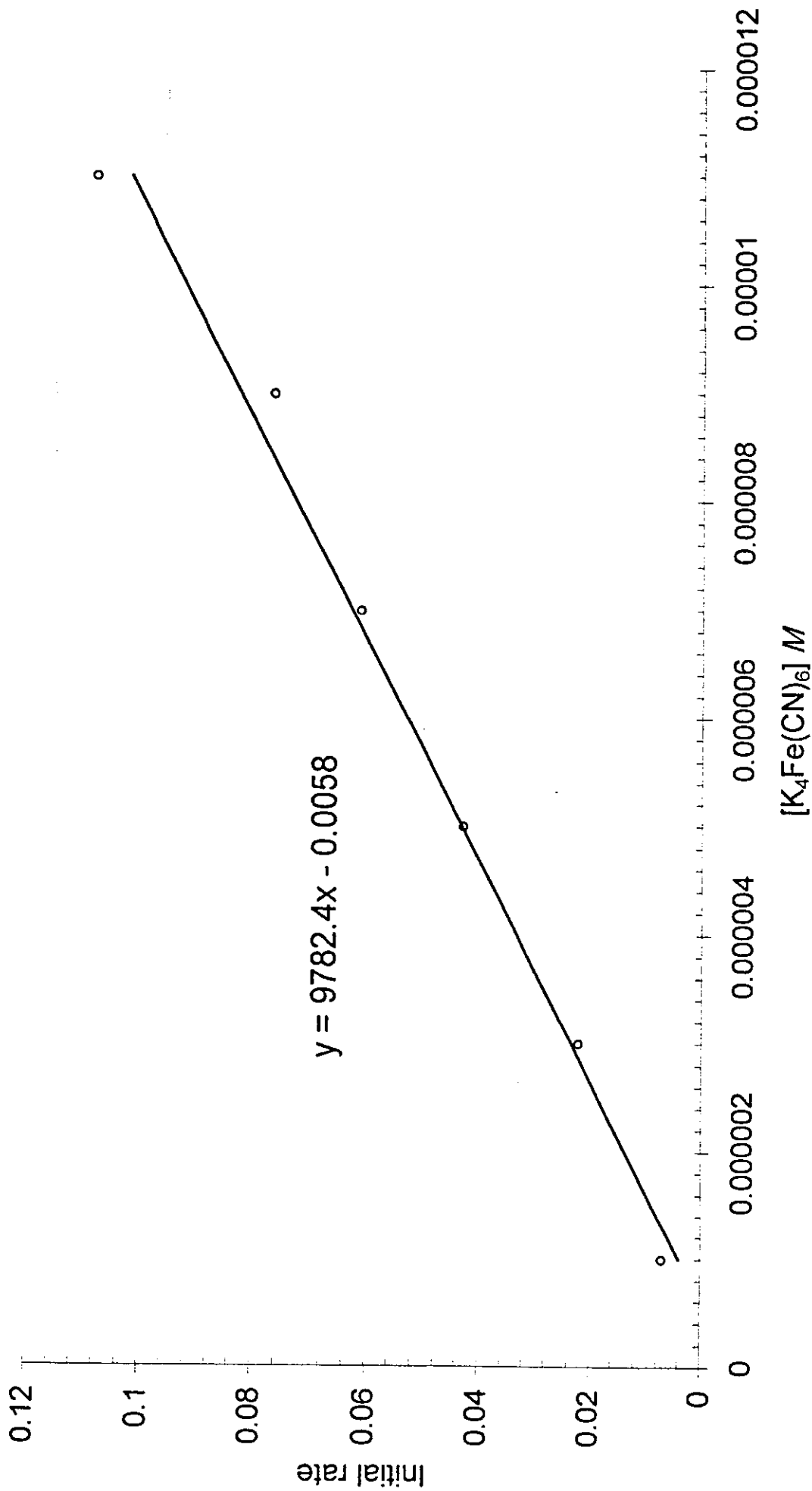


Figure (3.13): A plot of Initial rate vs. $[\text{K}_4\text{Fe}(\text{CN})_6]$
 $[\text{Ferene}] = 0.8 \times 10^{-3} \text{ M}$, $[\text{HgCl}_2] = 0.8 \times 10^{-4} \text{ M}$, $[\text{KNO}_3] = 0.1 \text{ M}$, $T = 40^\circ \text{ C}$, $\text{pH} = 3$

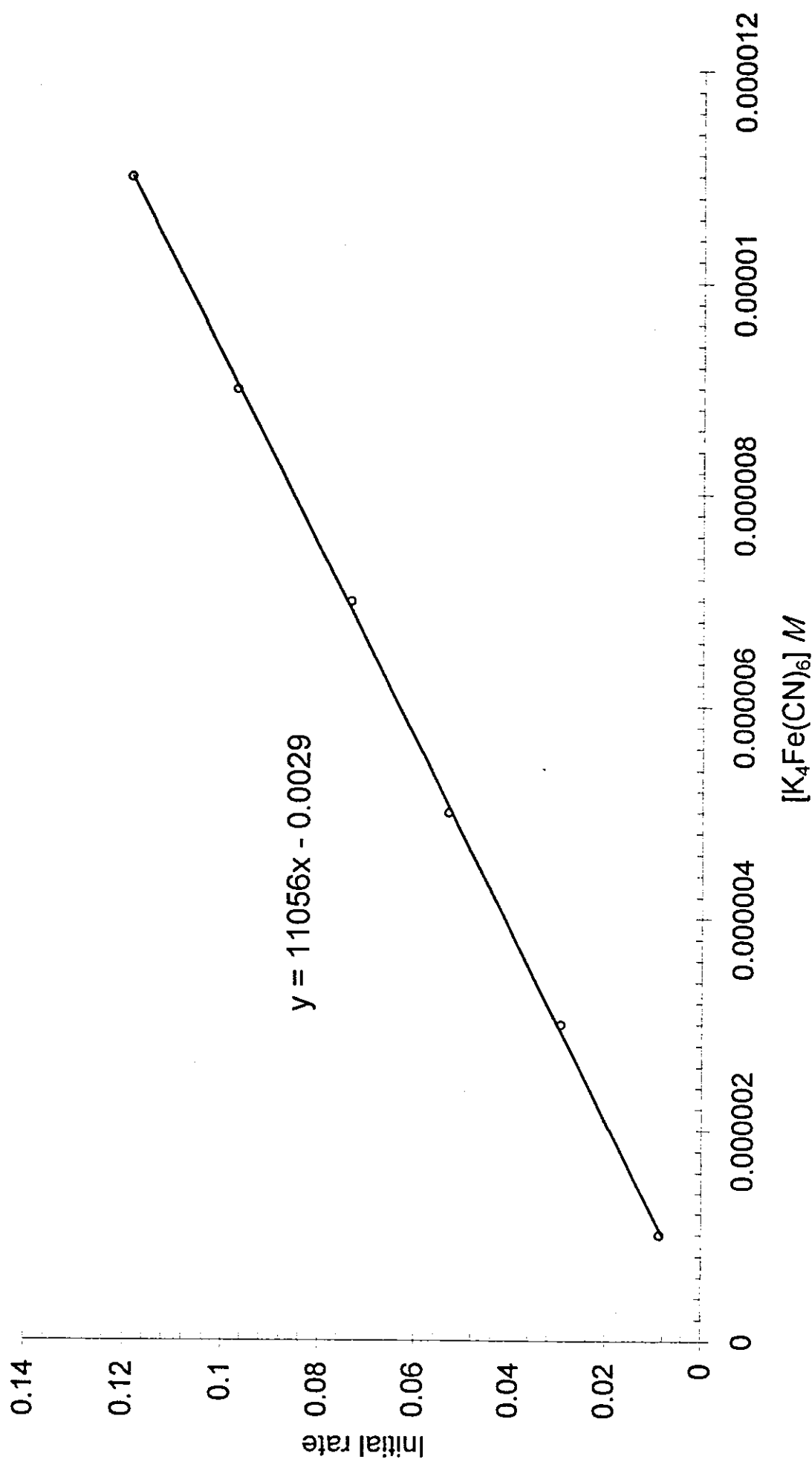


Figure (3.14): A plot of Initial rate vs. [K₄Fe(CN)₆]
[Ferene] = 0.8x10⁻³ M, [HgCl₂] = 0.8x10⁻⁴ M, [KNO₃] = 0.1 M, T = 50 °C, pH = 3

Table (3.10): Effect of temperature on the reaction rate of the substitution of cyanide in potassium hexacyanoferrate(II) by Ferene S in presence of HgCl_2 catalyst.

$T(^{\circ}\text{C})$	$T(^{\circ}\text{K})$	k_{obs} (s^{-1})	$1/T \times 10^{-3}$ ($^{\circ}\text{K})^{-1}$	$\ln(k_{\text{obs}})$
15	288	0.00034	3.472	-7.986
25	298	0.001249	3.356	-6.685
30	303	0.002375	3.300	-6.043
40	313	0.004593	3.195	-5.383
50	323	0.005191	3.096	-5.261

Conditions

$$[\text{Ferene S}] = 0.8 \times 10^{-3} \text{ M}$$

$$\text{pH} = 3 \pm 0.1$$

$$[\text{HgCl}_2] = 0.8 \times 10^{-4} \text{ M}$$

$$\lambda_{\text{max}} = 593 \text{ nm}$$

$$[\text{KNO}_3] = 0.1 \text{ M}$$

$$T = 15\text{-}50.0 \pm 0.1^{\circ}\text{C}$$

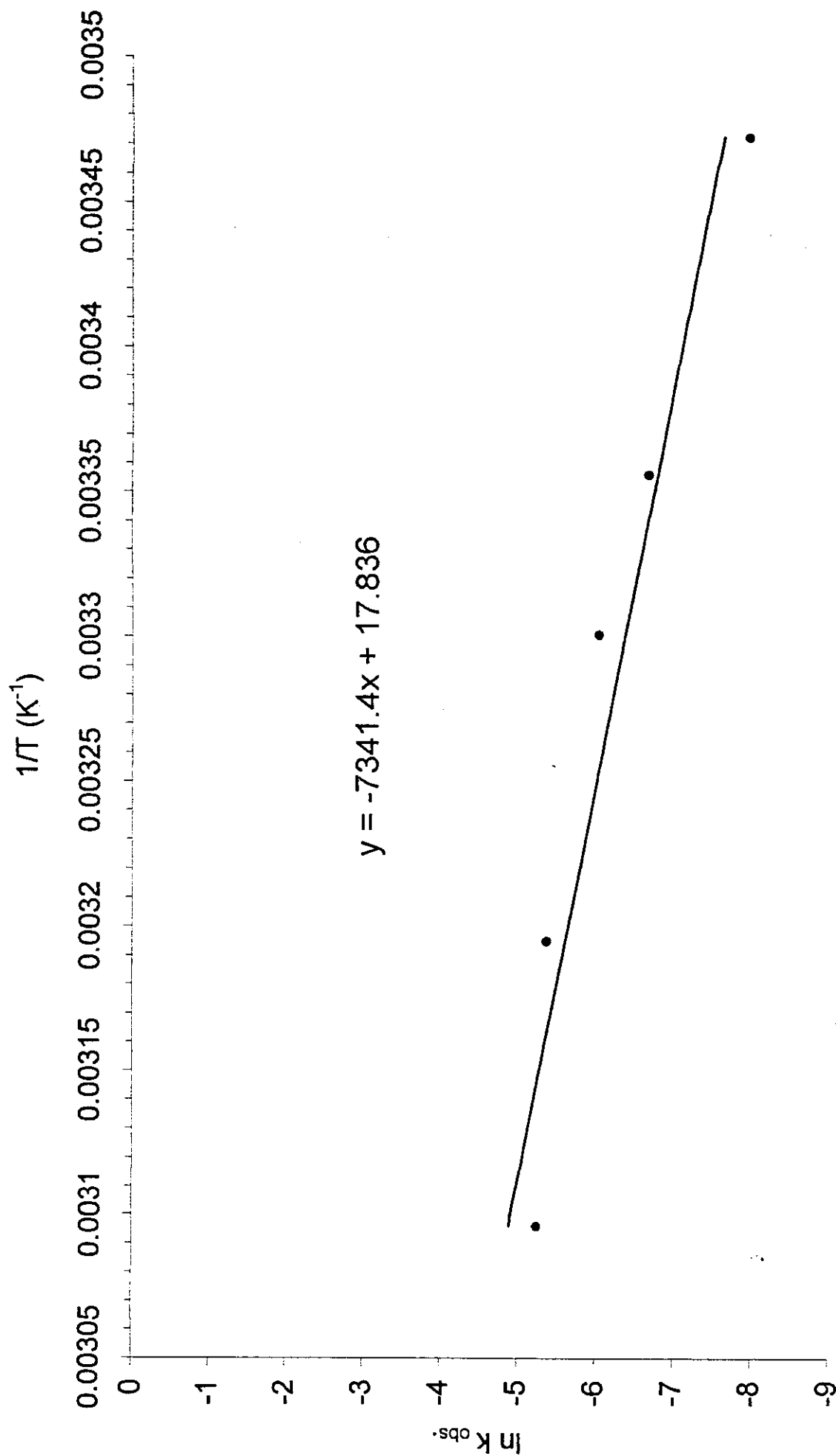


Fig (3.15): A plot of $\ln k_{obs}$ vs. $1/T$

[Ferene] = $0.8 \times 10^{-3} \text{ M}$, $[\text{HgCl}_2] = 0.8 \times 10^{-4} \text{ M}$, $[\text{KNO}_3] = 0.1 \text{ M}$, $\text{pH} = 3$

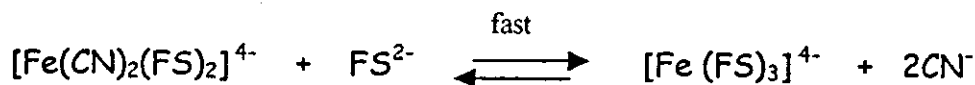
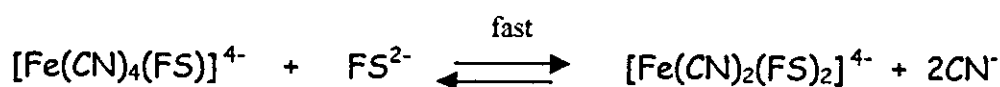
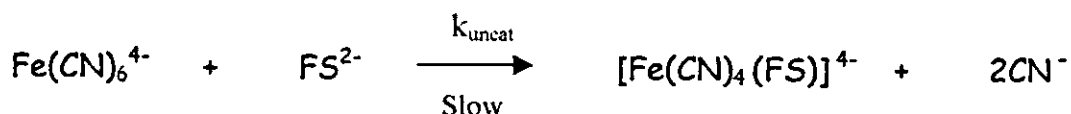
Table (3.11): The activation parameters for the substitution of CN^- in hexacyanoferrate(II) by Ferene S in presence of mercuric chloride catalyst at temperature of 25 °C.

The activation parameter		Value
Activation Energy	E_a^*	61.036 KJ/mol
Entropy Change	ΔS^*	-984.6 J/mol . °K
Enthalpy Change	ΔH^*	58.559 KJ/mol
Gibbs Free Energy	ΔG^*	351.986 KJ/mol

[3.8] The reaction mechanism and rate law:

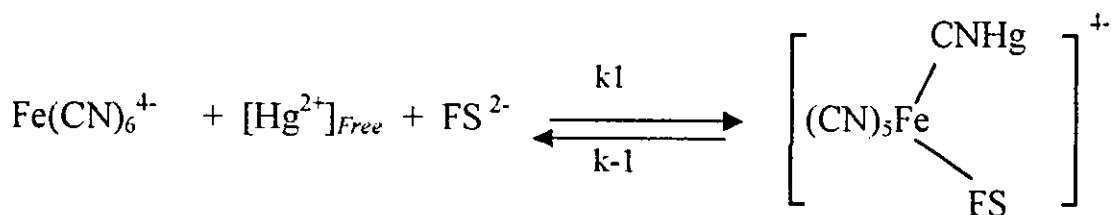
From experimental data and observations obtained during the experimental work the following mechanism is postulated that yields a rate law compatible with experimental observation:

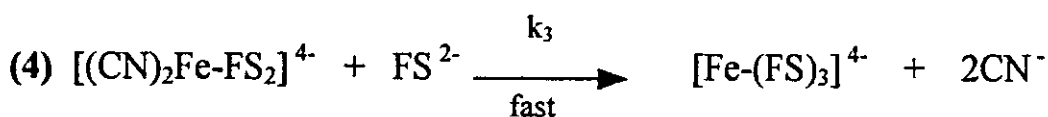
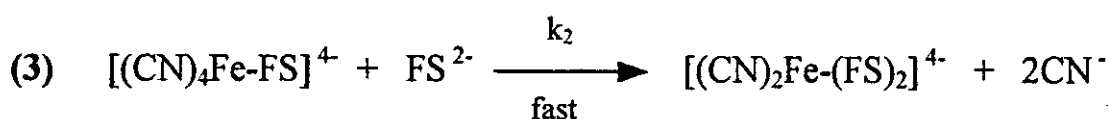
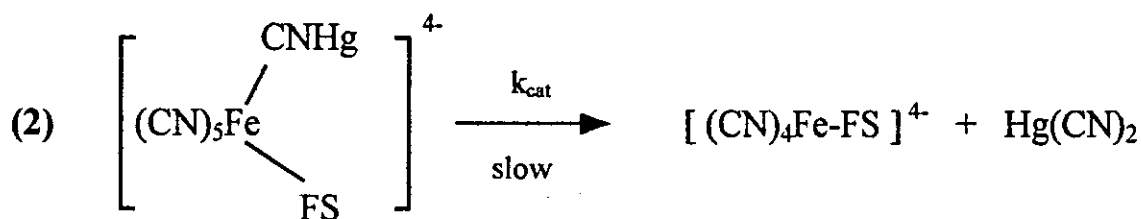
The uncatalyzed reaction mechanism:



The catalyzed reaction mechanism:

The following steps are proposed to be the elementary steps for the catalyzed mechanism:



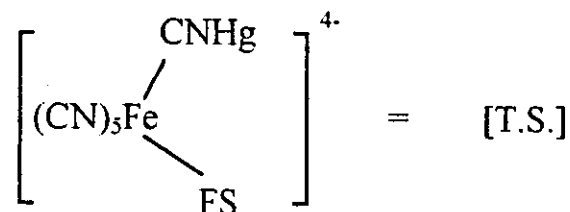


The rate law:

The rate law consists of two terms, the first one is the uncatalyzed reaction term and the other is the catalyzed reaction term, that is:

$$\text{Rate} = k_{\text{uncat}} [\text{Fe}(\text{CN})_6^{4-}] [\text{FS}^{2-}] + k_{\text{cat}} \left[\begin{array}{c} \text{CNHg} \\ \diagup \\ (\text{CN})_5\text{Fe} \\ \diagdown \\ \text{FS} \end{array} \right]^{4-}$$

Let



$$\text{Rate} = k_{\text{uncat}} [\text{Fe}(\text{CN})_6^{4-}] [\text{FS}^{2-}] + k_{\text{cat}} [\text{T.S.}] \quad \text{Equation (3.9)}$$

Using Steady state Approximation for [T.S.] we get:

$$k_1 [\text{Fe}(\text{CN})_6^{4-}] [\text{Hg}^{2+}]_{\text{Free}} [\text{FS}^{2-}] - k_{-1} [\text{T.S.}] - k_{\text{cat}} [\text{T.S.}] = 0$$

$$k_1 [\text{Fe}(\text{CN})_6^{4-}] [\text{Hg}^{2+}]_{\text{Free}} [\text{FS}^{2-}] = k_{-1} [\text{T.S.}] + k_{\text{cat}} [\text{T.S.}]$$

The total concentration of $[\text{Hg}^{2+}]_{\text{Total}}$ is present as

$$[\text{Hg}^{2+}]_{\text{Total}} = [\text{Hg}^{2+}]_{\text{Free}} + [\text{T.S.}]$$

$$[\text{Hg}^{2+}]_{\text{Free}} = [\text{Hg}^{2+}]_{\text{Total}} - [\text{T.S.}]$$

Substituting for $[\text{Hg}^{2+}]_{\text{Free}}$ gives:

$$k_1 [\text{Fe}(\text{CN})_6^{4-}] [\text{FS}^{2-}] \left[[\text{Hg}^{2+}]_{\text{Total}} - [\text{T.S.}] \right] = \left[k_{-1} + k_{\text{cat}} \right] [\text{T.S.}]$$

$$\begin{aligned} k_1 [\text{Fe}(\text{CN})_6^{4-}] [\text{FS}^{2-}] [\text{Hg}^{2+}]_{\text{Total}} \\ = [k_{-1} + k_{\text{cat}}] [\text{T.S.}] + k_1 [\text{Fe}(\text{CN})_6^{4-}] [\text{FS}^{2-}] [\text{T.S.}] \end{aligned}$$

$$k_1 [\text{Fe}(\text{CN})_6^{4-}] [\text{FS}^{2-}] [\text{Hg}^{2+}]_{\text{Total}} = \left[k_{-1} + k_{\text{cat}} + k_1 [\text{Fe}(\text{CN})_6^{4-}] [\text{FS}^{2-}] \right] [\text{T.S.}]$$

Solving for [T.S.] we have:

$$[\text{T.S.}] = \frac{k_1 [\text{Fe}(\text{CN})_6^{4-}] [\text{FS}^{2-}] [\text{Hg}^{2+}]_{\text{Total}}}{k_{-1} + k_{\text{cat}} + k_1 [\text{Fe}(\text{CN})_6^{4-}] [\text{FS}^{2-}]}$$

Substituting for [T.S.] in *Equation (3.9)* we get:

$$\text{Rate} = k_{\text{uncat}} [\text{Fe}(\text{CN})_6^{4-}] [\text{FS}^{2-}] + \frac{k_{\text{cat}} k_1 [\text{Fe}(\text{CN})_6^{4-}] [\text{FS}^{2-}] [\text{Hg}^{2+}]_{\text{Total}}}{k_{-1} + k_{\text{cat}} + k_1 [\text{Fe}(\text{CN})_6^{4-}] [\text{FS}^{2-}]}$$

Dividing both the denominator and the nominator by k_{-1} and recalling that $K_{\text{eq}} = k_1 / k_{-1}$

Equation (3.10)

$$\text{Rate} = k_{\text{uncat}} [\text{Fe}(\text{CN})_6^{4-}] [\text{FS}^{2-}] + \frac{k_{\text{cat}} K [\text{Fe}(\text{CN})_6^{4-}] [\text{FS}^{2-}] [\text{Hg}^{2+}]_{\text{Total}}}{1 + \frac{k_{\text{cat}}}{k_{-1}} + K [\text{Fe}(\text{CN})_6^{4-}] [\text{FS}^{2-}]}$$

[3.9] The rate constants:

Case (I): low concentration of $K_4Fe(CN)_6$ and Ferene

In this case the dominator will be approximately unity and hence the rate law could be reduced to:

$$\begin{aligned} \text{Rate} &= k_{uncat} [Fe(CN)_6^{4-}] [FS^{2-}] + k_{cat} K [Fe(CN)_6^{4-}] [FS^{2-}] [Hg^{2+}]_{Total} \\ &= (k_{uncat} [FS^{2-}] + k_{cat} K [FS^{2-}] [Hg^{2+}]_{Total}) [Fe(CN)_6^{4-}] \quad \text{Equation (3.11)} \end{aligned}$$

where

$$k_{obs} = k_{uncat} [FS^{2-}] + k_{cat} K [FS^{2-}] [Hg^{2+}]_{Total} \quad \text{Equation (3.12)}$$

Thus Equation (3.12) reduced to:

$$\text{Rate} = k_{obs} [Fe(CN)_6^{4-}] \quad \text{Equation (3.13)}$$

Therefore the above mechanism predicts that the reaction obeys first order kinetics with respect to each of hexacyanoferrate(II), Ferene, and mercury(II) catalyst. This can only happen at low concentration of $K_4Fe(CN)_6$ and Ferene.

Case (II): High concentration of $K_4Fe(CN)_6$ and Ferene

In this case since $K [Fe(CN)_6^{4-}] [FS^{2-}] \gg 1 + \frac{k_{cat}}{k_{-1}}$

Then the rate will be

$$Rate = k_{uncat} [Fe(CN)_6^{4-}] [FS^{2-}] + \frac{k_{cat} K [Fe(CN)_6^{4-}] [FS^{2-}] [Hg^{2+}]_{Total}}{1 + \frac{k_{cat}}{k_{-1}} + K [Fe(CN)_6^{4-}] [FS^{2-}]}$$

$$Rate = k_{uncat} [Fe(CN)_6^{4-}] [FS^{2-}] + k_{cat} [Hg^{2+}]_{Total} \quad \text{Equation (3.14)}$$

As shown above, the derived rate law predict that, at high concentrations of hexacyanoferrate(II) and Ferene the order of the reaction would be zero with respect to hexacyanoferrate(II), and Ferene. This result was proved experimentally as shown in figure (3.6) for $K_4Fe(CN)_6$ and figure (3.7) for Ferene.

The rate constants:

Upon plotting Equation (3.14), that is the initial rate against $[Hg^{2+}]$ a straight line was obtained in which the slope = k_{cat} , and the intercept is equal to $k_{uncat} [Fe(CN)_6^{4-}] [FS^{2-}]$

Also plotting *Equation (3.13)*, that is the initial rate against $[\text{K}_4\text{Fe}(\text{CN})_6]$, a straight line with slope = k_{obs} , is obtained.

The value of the equilibrium constant, K , can be calculated by substituting the values of k_{cat} , k_{obs} , and k_{uncat} in *Equation (3.12)* above.

The results are tabulated below at 25 °C table (3.12). The same calculations are repeated at other temperatures.

Table (3.12): The calculated rate constants:

k_{cat}	$1.364 \times 10^{-2} \text{ s}^{-1}$
k_{uncat}	$2.04 \times 10^{-3} \text{ M}^{-1} \text{ s}^{-1}$
k_{obs}	$2.18 \times 10^{-3} \text{ s}^{-1}$
K_{eq}	15.967×10^5

Atypical Calculation at 25 °C:

The plot of initial rate versus $[\text{HgCl}_2]$ gave a slope of **29063**, and an intercept of **0.0557** as shown in figure (3.17). Conversion of the slope and intercept to molar units and seconds is accomplished by dividing by the extinction coefficient of $35500 \text{ L cm}^{-1} \text{ mol}^{-1}$ and 60.

$$\text{Slope} = k_{cat} = \frac{29063}{35500 \times 60} = 1.364 \times 10^{-2} \text{ s}^{-1}$$

$$\text{Intercept} = k_{uncat} [\text{Fe}(\text{CN})_6^{4-}] [\text{Ferene}]$$

$$\frac{\text{Intercept}}{35500 \times 60} = k_{uncat} [\text{Fe}(\text{CN})_6^{4-}] [\text{Ferene}]$$

$$\frac{0.0557}{35500 \times 60} = k_{uncat} [\text{Fe}(\text{CN})_6^{4-}] [\text{Ferene}]$$

Substituting the values of the concentrations yields

$$k_{uncat} = 2.04 \times 10^{-3} \text{ M}^{-1} \text{ s}^{-1}$$

This value of k_{uncat} deduced by the rate law derived for the mechanism agrees in an excellent way with the experimental k_{uncat} where the experimental k_{uncat} derived from figure (3.3) is $= 2.034 \times 10^{-3} \text{ M}^{-1} \text{ s}^{-1}$

This is an indication that approves and confirms the mechanism.

Table (3.13): Effect of lower concentrations of $[\text{K}_4\text{Fe}(\text{CN})_6]$ on the rate law.

$[\text{K}_4\text{Fe}(\text{CN})_6]$ M	Initial Rate (min^{-1})	$[\text{K}_4\text{Fe}(\text{CN})_6]$ M	Initial Rate (min^{-1})
1×10^{-6}	0.00075	10×10^{-6}	0.0489
5×10^{-6}	0.01875	20×10^{-6}	0.09355
7×10^{-6}	0.03275	30×10^{-6}	0.136
8×10^{-6}	0.03895		

Conditions :

$$[\text{K}_4\text{Fe}(\text{CN})_6] = 1 \times 10^{-6} \text{ — } 30 \times 10^{-6} M$$

$$\text{pH} = 3 \pm 0.1$$

$$[\text{Ferene S}] = 1 \times 10^{-3} M$$

$$\lambda_{\text{max}} = 593 \text{ nm}$$

$$[\text{HgCl}_2] = 1 \times 10^{-4} M$$

$$T = 25.0 \pm 0.1 \text{ } ^\circ\text{C}$$

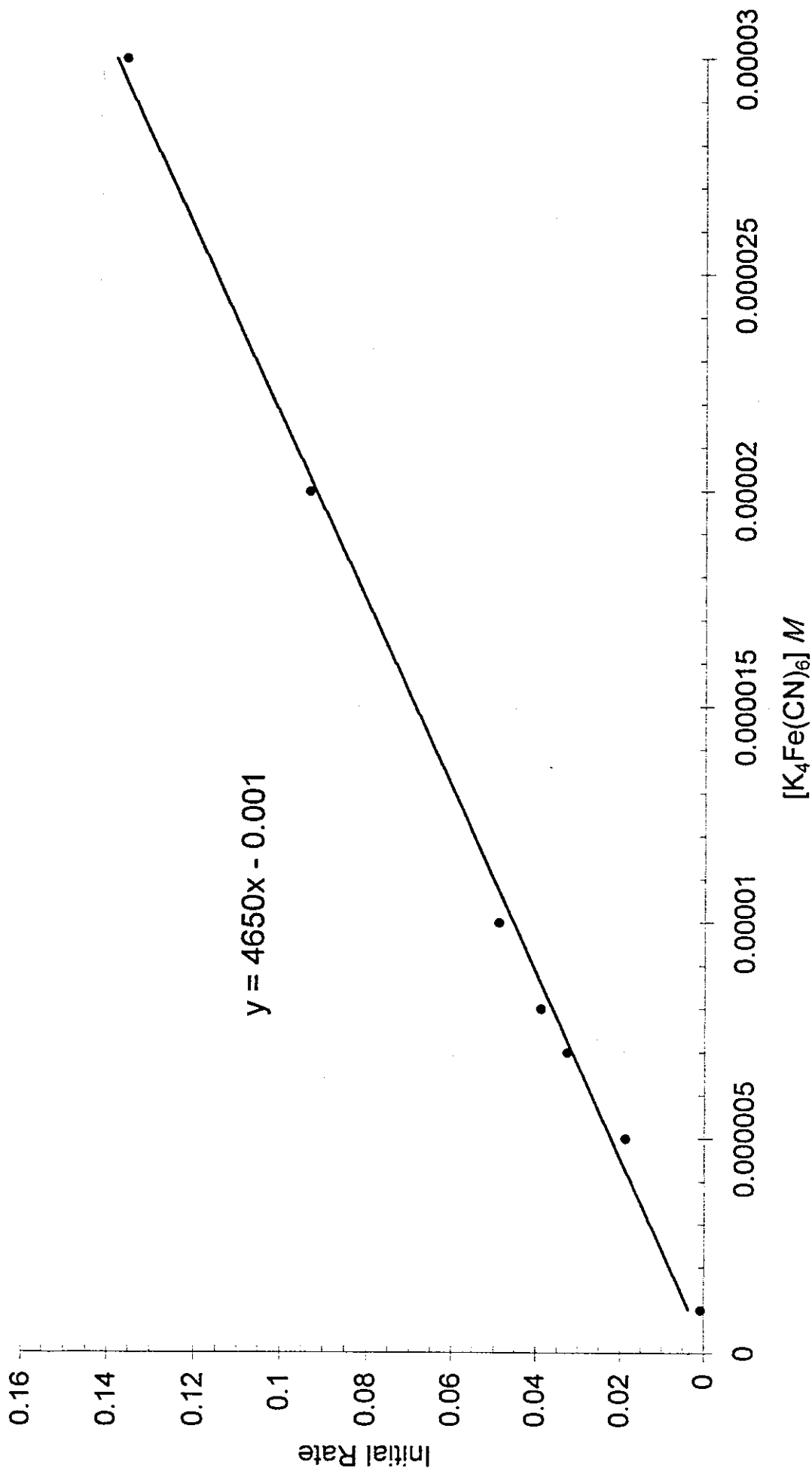


Figure (3.16): A plot of Initial rate vs. $[K_4Fe(CN)_6]$
 $[Ferene] = 1 \times 10^{-3} M$, $[HgCl_2] = 1 \times 10^{-4} M$, $T = 25^\circ C$, $pH = 3$

Table (3.14): Effect of high concentration of [K₄Fe(CN)₆] and [Ferene]on the rate law at different HgCl₂ concentrations.

[HgCl ₂] <i>M</i>	Initial Rate (<i>min</i> ⁻¹)
0.00000016	0.06115
0.00000032	0.06765
0.0000004	0.0611
0.00000056	0.07455

Conditions :

[K₄Fe(CN)₆] = 1.6 x10⁻³ *M*

pH = 3 ± 0.1

[Ferene S] = 8 x10⁻³ *M*

λ_{max} = 593 nm

[KNO₃] = 0.1 *M*

T = 25.0 ± 0.1 °C

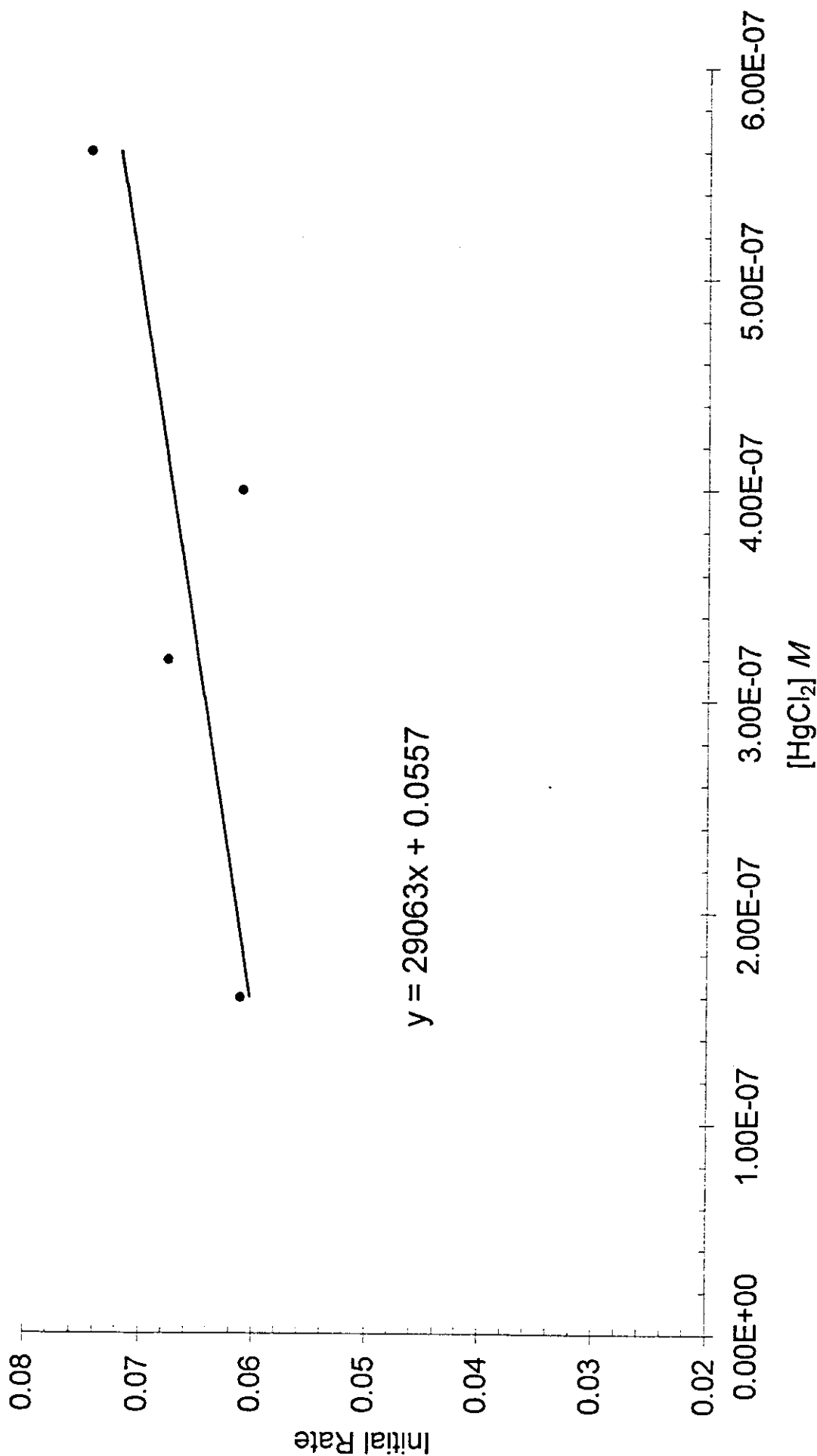


Figure (3.17): A plot of Initial rate vs. [HgCl₂] at high concentrations of [K₄Fe(CN)₆] and Ferene
 [K₄Fe(CN)₆] = 1 × 10⁻⁴ M, [Ferene] = 1 × 10⁻³ M, [KNO₃] = 0.1 M, pH = 3, T = 25° C.

[3.10] Calibration graph:

Upon inspection for the relationship between mercury(II) concentration and the complex absorbance, a linear curve was obtained within the range 0.5-20 ppm of mercury(II). The calibration curve was determined under the following conditions:

$$[K_4Fe(CN)_6] = 1 \times 10^{-4} M$$

$$pH = 3 \pm 0.1$$

$$[Ferene S] = 1 \times 10^{-3} M$$

$$\lambda_{max} = 593 \text{ nm}$$

$$T = 25.0 \pm 0.1 \text{ } ^\circ\text{C}$$

$$\text{Time} = 5 \text{ min}$$

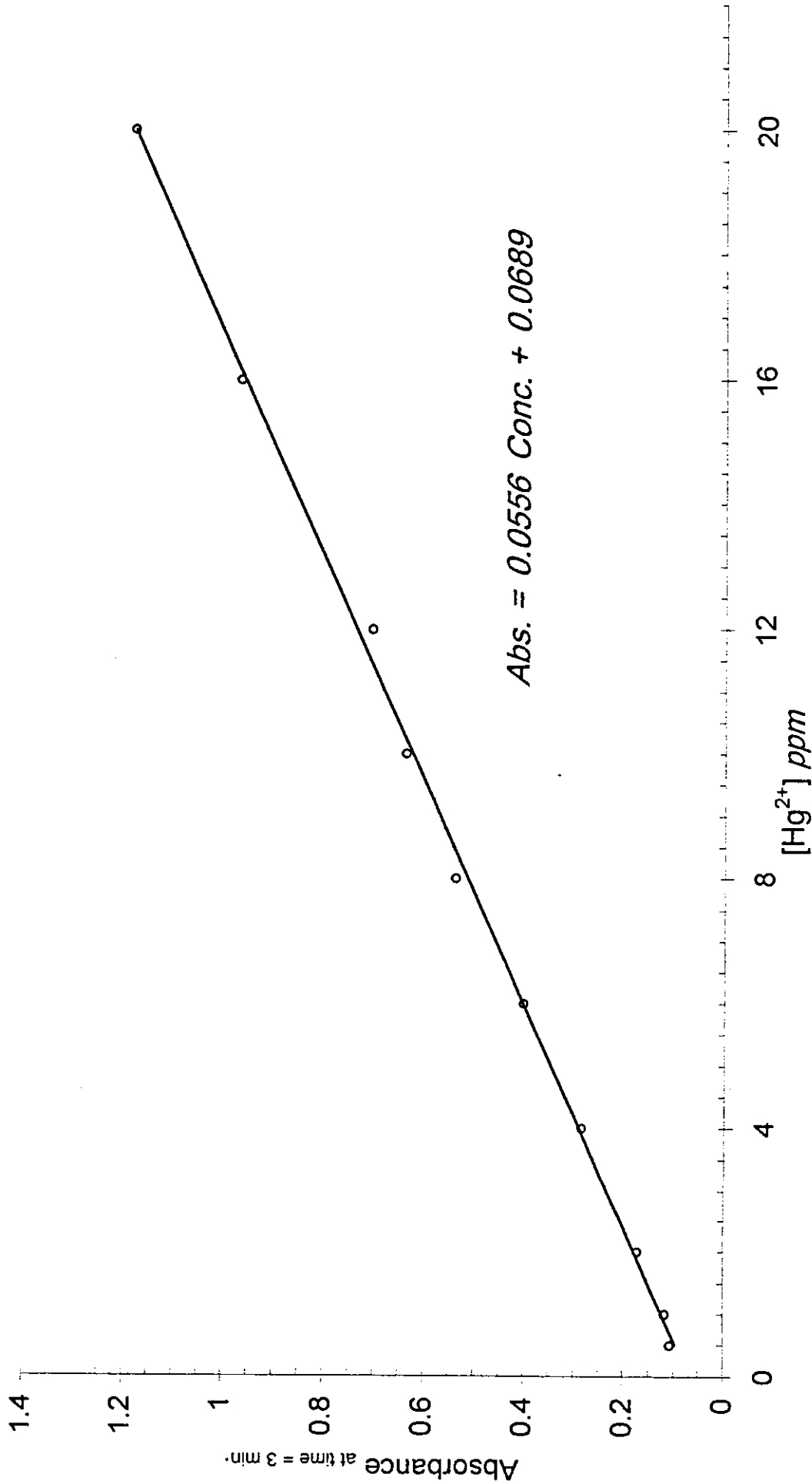
$$[Hg^{2+}] = 0.5 - 20 \text{ ppm}$$

The results are tabulated in table (3.15) and shown graphically in figure (3.18)

Table (3.15): The Calibration graph data:

$[Hg^{2+}] \text{ ppm}$	Absorbance*	$[Hg^{2+}] \text{ ppm}$	Absorbance*
0.5	0.1071	8	0.537
1	0.1176	10	0.6372
2	0.1724	12	0.7041
4	0.2855	16	0.9661
6	0.4003	20	1.1798

* The absorbance was measured after 3 minutes



Figure(3.18): Calibration Curve for $[\text{Hg}^{2+}]$ in ppm

$[\text{K}_4\text{Fe}(\text{CN})_6] = 1 \times 10^{-4} \text{ M}$, $[\text{Ferene}] = 1 \times 10^{-3} \text{ M}$, $\text{pH} = 3$, $T = 25^\circ \text{C}$.

[3.11] Effect of Foreign ions:

The effect of foreign ions was investigated for different cations and anions.

By studying table (3.16). In general monovalent cations like Na, K, Ag, and bivalent cations of the alkaline earth metals do not interfere appreciably. Bivalent cations like Zn, Cd, and Ni interfere seriously. A. Bellomo reports the possibility of the hexacyanoferrate(II) ion react with a metallic bivalent ion M(II) as shown:



Also formation of $K_2M_2[Fe(CN)_6]_2$ is possible. These complexes lead to a shortage of the hexacyanoferrate species needed for ferrous-Ferene complex.

Concerning the anions Nitrate, Sulfate and Acetate do not interfere, but most interference was for Iodine ion. The results of the foreign ions are reported in table (3.16)

Table (3.16): Effect of foreign cations and anions on the absorbance using 20 ppm of Hg(II)

Foreign ion	Foreign ion Concentration <i>ppm</i>	Ion:Hg(II) Mass ratio	Absorbance	% Error
No ions present	—	—	1.31	—
Na(I)	100	5:1	1.29	-1.5
K(I)	160	8:1	1.34	+2.3
Ag(I)	250	12.5:1	1.52	+16
	25	1.25:1	1.39	+6.1
	12.5	0.625:1	1.36	+3.8
Mg(II)	250	12.5:1	1.25	-6.1
Zn(II)	250	12.5:1	0.03	-97.7
	25	1.25:1	0.04	-96.9
	12.5	0.625:1	0.38	-71
Cd(II)	250	12.5:1	0.09	-93.1
	25	1.25:1	0.6	-54.2
	12.5	0.625:1	0.82	-37.4
Ni(II)	250	12.5:1	0.03	-97.1
	25	1.25:1	0.536	-59.1
Co(II)	250	12.5:1	0.12	-90.1
	25	1.25:1	0.86	-34.4
Cu(II)	250	12.5:1	0.09	-93.1
	25	1.25:1	1.13	-13.7
NO ₃ ⁻	250	12.5:1	1.34	+2.3
Cl ⁻	250	12.5:1	0.91	-30.5

SO_4^{2-}	1000	50:1	1.23	-6.1
CH_3COO^-	250	12.5:1	1.29	-1.5
I^-	250	12.5:1	0.02	-98.5
	25	1.25:1	0.44	-66.4

Conditions :

$$[\text{K}_4\text{Fe}(\text{CN})_6] = 1 \times 10^{-4} \text{ M}$$

$$\text{pH} = 3 \pm 0.1$$

$$[\text{Ferene S}] = 1 \times 10^{-3} \text{ M}$$

$$\lambda_{\text{max}} = 593 \text{ nm}$$

$$T = 25.0 \pm 0.1 \text{ } ^\circ\text{C}$$

$$\text{Time} = 5 \text{ min}$$

$$[\text{HgCl}_2] = 1 \times 10^{-4} \text{ M} \cong 20 \text{ ppm of Hg(II)}$$

[3.12] Application:

The mercury content in medical sample that contains mercury -(an Israeli hand cream under commercial name "Bleaching Cream")- has been done using about 3 grams of the medical sample and following the general procedure described previously for treatment of sample. The absorbance of the medical sample shows that this sample contains an average value of about 1.85 mg Hg^{2+} /1g of sample. The results obtained are shown in table (3.17) below.

Table (3.17): Calculated mercury(II) content in a medicinal sample:

Run Number	Absorbance*	Determined Concentration <i>ppm</i>
1	0.1096	0.73
2	0.0983	0.53
3	0.0913	0.4
4	0.0981	0.53
5	0.1025	0.6
6	0.0996	0.55
7	0.0995	0.55
<i>The Average Concentration</i>		0.556

* The absorbance was measured after 3 minutes

Conditions :

$$[\text{K}_4\text{Fe}(\text{CN})_6] = 1 \times 10^{-4} \text{ M}$$

$$\text{pH} = 3 \pm 0.1$$

$$[\text{Ferene S}] = 1 \times 10^{-3} \text{ M}$$

$$\lambda_{\text{max}} = 593 \text{ nm}$$

$$T = 25.0 \pm 0.1 \text{ } ^\circ\text{C}$$

REFERENCES:

1. J. D. Artiss, S. Vinograov, and B. Zak, *Clin. Biochem.* **14** (6) 311-315 (1981).
2. J. D. Artiss, D. R. Strandbergh, and B. Zak, *Microchemical Journal*, **28**, 275-284, (1983)
3. D. J. Hennessy, G. R. Reid, F. E. Smith, and S. L., Thompson *Can. J. Chem.*, **62**, 721-724, (1984)
4. G. Lindstedt, *Analyst*, **95**, 264-271, (1970)
5. G. Lindstedt and I. Skare, *Analyst*, **96**, 223-229, (1971)
6. I. Skare, *Analyst*, **97**, 148-155, (1972)
7. T. P. Ruiz, J. A. Ortuno and C. S. Perdreno, *Analyst*, **109**, 1581-1583, (1984).
8. B. F. Shraydeh, A. Z. Abu Zuhri, M. A. Hannoun, *Spect. Lett.*, **19**, 929,(1986).
9. Y. Anjaneyulu, P. C. Mouli, M. R. P. Reddy and K. P. C. Sekhar *Analyst*, **110**, 391-401, (1985).
10. E. B. Swain, D. R. Engstrom, M. E. Brigham, T. A. Henning, and P. L. Brezonik, *Science*, **272**, 784-787, (1992)
11. B. F. Shraydeh, M. Abu-Eid, N. A. Zatar, I. Shakhshier, and M. Khamis, *Main Group Metal Chemistry*, **19/2**, 103-106, (1996).
12. I. V. Dragojević, D. Dragojević and S. Čadež, *Analytica Chimica Acta*, **355**, 151-156, (1997)
13. K. I. Al-Taradee, *M. Sc. Thesis*, An-Najah National University, (1997).

14. B. Douglas, D. H. McDaniel, and J. J. Alexander, *Concepts and Models of Inorganic Chemistry*, 2nd ed., John Wiley & Sons, Inc., New York, (1983).
15. J. E. Brady, *General Chemistry, Principles & Structure*, 5th ed., John Wiley & Sons, Inc., New York, (1990).
16. *Microsoft Bookshelf 98 Desk*, Microsoft Corporation, USA, (1998)
17. *Microsoft Encarta 98 Encyclopedia Desk*, Microsoft Corporation, USA, (1998)
18. B. G. Katzung, *Basic & Clinical Pharmacology*, 5th ed., Prentice Hall, Inc., New Jersey, (1992).
19. C. R. Gibbs, *Analytical Chemistry*, **48** (8), 1197-1200, (1976)
20. F. Ceriotti and G. Ceriotti, *Clin. Chem.*, **26/2**, 327-331, (1980)
21. S. Ašperger, I. Murati, and O. Čupahin *J. Chem. Soc.*, 1041-1046, (1953)
22. S. Ašperger, and I. Murati, *Anal. Chem.*, **23**, 513, (1954)
23. S. Ašperger, and D. Pavlović, *J. Chem. Soc.*, 1449-1454, (1955).
24. S. Ašperger, I. Murati, and D. Pavlović, *J. Chem. Soc. (A)*, 2044-2047, (1969)
25. M. Phull and P. C. Nigman, *Talanta*, **23**, 591-597, (1981)
26. S. Ramna, *J. Inorg. Anal. Chem.* **43**, 1855-1858, (1981).
27. D. A. Skoog, D. M. West, and F. J. Holler, *Fundamentals of Analytical Chemistry*, 6th ed., Saunders College Publishing, Florida, (1992).
28. G. L. Traister and A. A. Schilt, *Anal. Chem.*, **48** (4), 513, (1976)
29. M. T. Beck and E. C. Porzolt, *J. Coord. Chem.*, **1**, 57, (1971).
30. H. E. Avery, *Basic reaction kinetics and mechanisms*, 2nd ed., John Wiley & Sons, Inc., New York, (1961).

31. A. A. Frost and R. G Pearson, *kinetics and mechanism*, 2nd ed., John Wiley & Sons, Inc., New York, (1961).
32. R. Weston, Jr. and H. A. Schwarz, *Chemical Kinetics*, 10th ed., Prentice Hall, Inc., New Jersey, (1972).
33. G. W. Castellan, *Physical Chemistry*, 3rd ed., The Benjamin/Cumming Publishing Company, Inc., Sydney, (1983).
34. L. Z. Majjad, M. Sc. Thesis, An-Najah National University, (1997).
35. P. W. Atkins, *Physical Chemistry*, 6th ed., Oxford University Press, Oxford, (1998).
36. N. A. M. Turkman, M. Sc. Thesis, An-Najah National University, (1999).
37. K. B. Yatasimiriskii, *Kinetic Methods of Analysis*, Pergamon Press Ltd., Glasgow, (1966).
38. A. A. Frost and R. G. Pearson, *Kinetics and Mechanism*, 2nd ed. John Wiley & Sons, Inc. New York, (1961).
39. W.J. Popiel, *Laboratory Manual Of Physical Chemistry*, The English University Press LTD., London, (1964)
40. A. Bellomo, Talanta, 17, 1109-1114, (1970)
41. D. Nicholls, *Complexes and First-Row Transition Elements*, Macmillan Press, London, (1981).
42. S. D. Olsen, R. H. Filby, T. Brekke, G. H. Tsaksen, Analyst, 120, 1379, (1995).
43. J. Enzweiler, P. J. Potts, K. E. Jarvis, Analyst, 120, 1391, (1995).